RIGA TECHNICAL UNIVERSITY

Genādijs Kobenkins

THE ENSURING OF STABLE VIBRATION-STRENGTH INDICATORS OF GEARED TRACTION MOTORS IN VARIABLE FREQUENCY AND LOAD MODES

Summary of the Doctoral Thesis

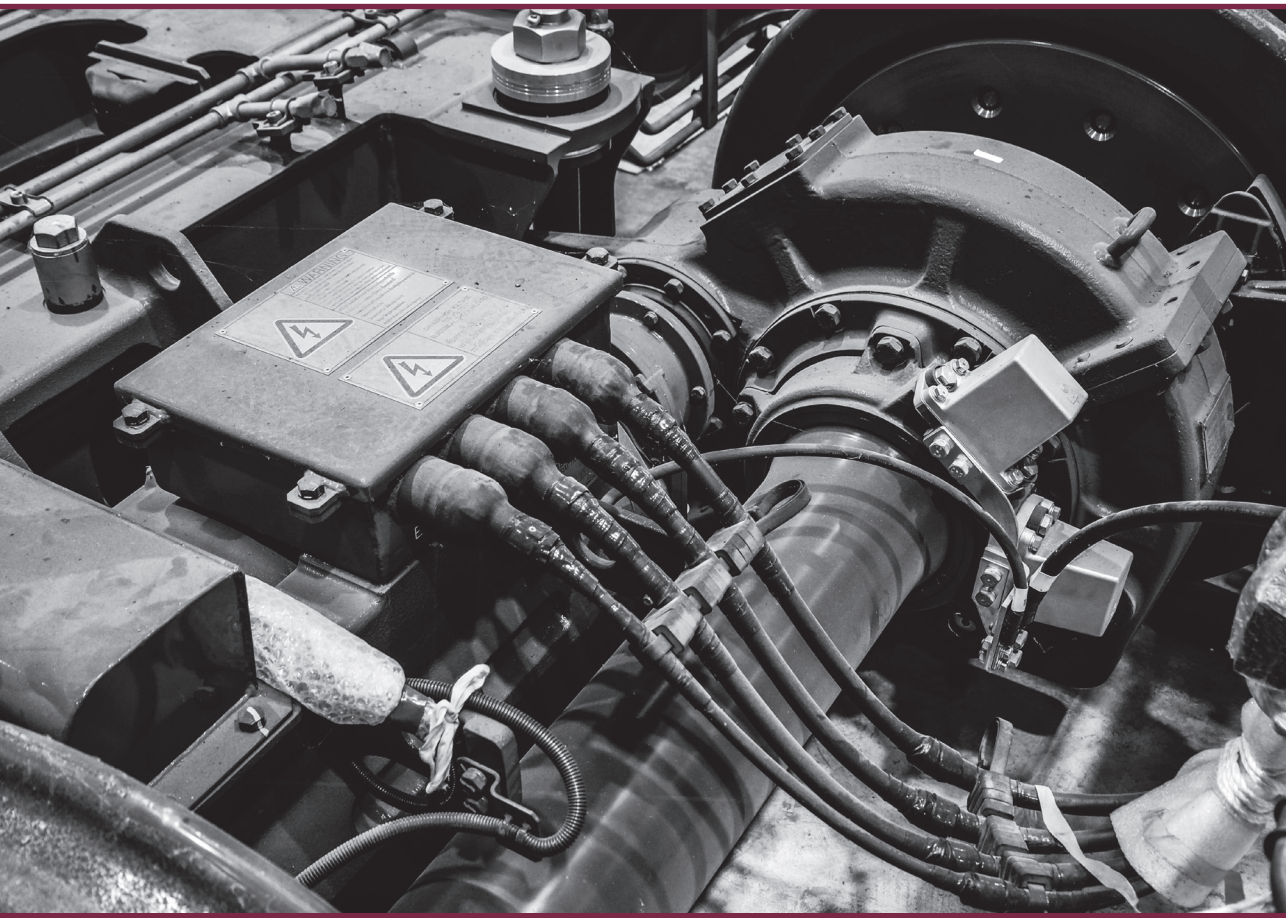

RTU Press
Riga 2025

RIGA TECHNICAL UNIVERSITY
Faculty of Computer Science, Information Technology and Energy
Institute of Industrial Electronics, Electrical Engineering and Energy

Genādijs Kobenkins
Doctoral Student of the Study Programme "Smart Power Systems"

THE ENSURING OF STABLE VIBRATION-STRENGTH INDICATORS OF GEARED TRACTION MOTORS IN VARIABLE FREQUENCY AND LOAD MODES

Summary of the Doctoral Thesis

Scientific supervisor:
Professor Dr. sc. ing.
ANDREJS PODGORNOVS
Scientific advisor:
Docent Dr. sc. ing.
OĻEGS SĻISKIS

RTU Press
Riga 2025

Kobenkins, G. The Ensuring of Stable Vibration-Strength Indicators of Geared Traction Motors in Variable Frequency and Load Modes. Summary of the Doctoral Thesis. – Riga: RTU Press, 2025. – 53 p.

Published in accordance with the decision of the Promotion Council P-05 of 17 December 2024, No. 105/24.

Cover picture from www.shutterstock.com.

https://doi.org/10.7250/9789934371424
ISBN 978-9934-37-142-4 (pdf)

DOCTORAL THESIS PROPOSED TO RIGA TECHNICAL UNIVERSITY FOR PROMOTION TO THE SCIENTIFIC DEGREE OF DOCTOR OF SCIENCE

To be granted the scientific degree of Doctor of Science (Ph. D.), the present Doctoral Thesis has been submitted for the defence at the open meeting of RTU Promotion Council on February 13, 2025 at 10.00 at the Faculty of Computer Science, Information Technology and Energy, Institute of Power Engineering of Riga Technical University, 12/1 Āzenes Street, Room 306.

OFFICIAL REVIEWERS

Professor Dr. habil. sc. ing. Antans Sauļus Sauhats
Riga Technical University, Latvia

Professor Ph.D. Loránd Szabó
Technical University of Cluj-Napoca, Romania

Associate Professor Ph.D. Zoltán Ádám Tamus
Budapest University of Technology and Economics, Hungary

DECLARATION OF ACADEMIC INTEGRITY

I hereby declare that the Doctoral Thesis submitted for review to Riga Technical University for promotion to the scientific degree of Doctor of Science (Ph. D) is my own. I confirm that this Doctoral Thesis has not been submitted to any other university for promotion to a scientific degree.

Genādijs Kobenkins ……. (signature)
Date: ……

The Doctoral Thesis has been written in English. It consists of an Introduction, 5 Chapters, Conclusion, 120 figures, and 28 tables; the total number of pages is 128. The Bibliography contains 136 titles.

CONTENTS

LIST OF ABBREVIATIONS

MGU – Motor Gear Unit
IM – Induction Motor
RMS – Root Mean Square
FFT – Fast Fourier Transform
DWT – Discrete Wavelet Transform
EMD – Empirical Mode Decomposition
EEMD – Ensemble Empirical Mode Decomposition
CEEMD – Complete Ensemble Empirical Mode Decomposition
HHT – Hilbert-Huang Transform
IMF – Intrinsic Mode Functions
IGBT – Insulated-Gate Bipolar Transistor
DTC – Direct Torque Control
PWM – Pulse Width Modulation
UMP – Unbalanced Magnetic Pull
MMF – Magnetomotive Force
EMF – Electromotive Force
EMU – Electric Multiple Unit
FEM – Finite Element Method
CW – Clockwise
CCW – Counterclockwise

GENERAL CHARACTERIZATION OF THE THESIS

Topic relevance

The relevance of the task is determined by the constant increase in passenger traffic and the continuous daily operation time of modern electrified rolling stock on suburban and regional routes. The main actuator of an electric train is an electric traction drive, complex in structure and a combination of mechanical, electromechanical and electronic devices united by a control system of the lower and upper levels. The tendency to develop and implement electric trains with an asynchronous traction drive to increase productivity during traffic intensification remains unchanged. The electric traction drive is an independent and complex system since the processes occurring in it have different physical natures and different natures of interaction and influence on each other. For enterprises operating in the industry of railway transport and transport electromechanical equipment, the main issue remains the release of high-quality and reliable products; especially this concerns a complex of enterprises producing products in a complete set, in most cases, the consumer is interested – the manufacturer of electric trains. It is clear from practice that the most common combination of an electric drive kit is most often represented by an actuator – a traction motor gear unit and a control mechanism – a traction converter for electric trains operating in a 3 kV network. For a 25 kV network, a traction transformer from the same manufacturer may also be included in the electrical equipment kit.

The basis for the release of high-quality and reliable products is compliance with technological processes according to the developed and implemented design documentation, as well as final acceptance tests, the scope of which is regulated by the current standards for the acceptance and operation of rolling stock. The main disadvantage of existing methods for testing electric drives is their disunity and the possibility of checking their interaction only as part of an electric train if we are talking about serial production and not experimental production. In this case, identifying and eliminating the causes of a malfunction becomes extremely difficult due to the frequent inaccessibility of actuators and the impossibility of identifying the true source of the malfunction.

The aim of the Doctoral Thesis

The Doctoral Thesis aims to study the readiness and technical condition of the actuator, namely the motor gear unit of the electric traction drive of a suburban and regional electric train at the stage of factory acceptance tests together with the supplied control system. It is an important task to implementat the proposed pre-operational tests of studies in the mode and under continuous production conditions, based on the creation of a methodology for an integrated approach to monitoring and analyzing the mechanical strength and vibration activity of traction equipment.

The following tasks were set and implemented within the framework of the Thesis research:

1. Develop a methodology for acceptance testing of traction geared motor together with an electric traction drive, taking into account the relationship of the traction and energy parameters of the geared motor unit with its vibration activity.

2. Determine the safety margin of the metal structure, taking into account the dynamic loads of the drive-in long-term loading modes and short-term maximum structural loads.

3. Detect defects by analyzing changes in diagnostic parameters and determine the correlations between them.

4. Test the methodology in industrial conditions based on a set of manufactured products, i.e., a set of electrical equipment submitted for testing and successfully tested in a 1 : 1 ratio before it is delivered to the customer.

As part of the Thesis research, an analysis was made of the results of studies on the problems of vibration states of transport and energy equipment, modern methods of mathematical modelling, and applied methods of diagnostics of electromechanical equipment.

Scientific novelty of the Thesis

1. The Thesis presents a study aimed at establishing the relationship between the dynamic-vibrational state of an object and its energy parameters, using the example of traction motor-gear units of electric trains. The presented methodology is aimed at the timely determination of technological deviations of serial samples and design flaws of new products.

2. The eccentricity of the air gap of an asynchronous motor, primarily affecting slip and, ultimately, the power factor, causes a change in the characteristics of the stator current, forming magnetic shocks of imbalance, leading to the vibration of the motor gear unit.

3. A method for determining the safety margin for the most visible design elements has been presented, considering dynamic loads on the motor gear unit.

Theoretical and practical significance of the Thesis

The method of monitoring the vibration condition of equipment is aimed at obtaining reliable results of acceptance tests and implementing the method of monitoring the technical condition of geared motor units operating as part of a train's electrical equipment complex under real operational loads.

The technique allows for the complete use of the information content of the electric motor energy indicators and the level of vibration disturbances of the geared motor unit during testing and, if necessary, significantly facilite the detection of faults.

The presented technique formed the basis of programs for acceptance of rotating units for the needs of rolling stock manufactured by JSC "Riga Electrical Machinery Factory".

Research methods, reliability and validity of results

The presented results of the Thesis research were obtained on the basis of the analysis of the functional features of asynchronous traction motors, the dynamics of traction drive loading and the conditions of their operation. The existing methods for solving the creation of a mechanical load on the shaft of the motor gear unit were carried out in laboratory and industrial conditions. A mechanical load control system was organized using the LabView software module. Based on a three-dimensional model of the motor gear unit with the help of a field solver, studies of the maximum stressed elements of the structure were carried out.

This Thesis research is presented in five chapters and chapter conclusions.

Chapter 1 provides an overview of current regulatory acts and documents and a list of regulatory standards related to the creation and control of the technical condition of products for rail transport. An overview of existing methods of applied vibration diagnostics is also given.

Chapter 2 provides an analysis of the physical relationships between normal and emergency operation of electric traction drives. The problems of vibration phenomena in rail transport are described. A mathematical description of the operation of gear motor units as part of an electric train drive is given.

Chapter 3 describes the operation of the traction geared motor unit and the forces acting on it and created inside it. The modes of checking the safety margin of the structure for further analysis of the critical stress of the geared motor unit housing and bearing seats are presented.

In Chapter 4, based on calculations of static and dynamic loads, an analysis of the stress of the motor gear unit structure is presented, and calculations are made to determine the safety margin of the structure.

In Chapter 5, the methodology is tested and the relationship between the vibration state of the equipment being tested and its energy indicators is established.

Approbation of the results

The results of the Thesis were presented at the following scientific conferences.

1. 17th Conference on Electrical Machines, Drives and Power Systems (ELMA 2021). Presentation: Carrying out of Tests for the Functionality of the Traction Autonomous Drives in the Conditions of Industry and Serial Production. Sofia, Bulgaria: IEEE, 2021.
2. 17th Conference on Electrical Machines, Drives and Power Systems (ELMA 2021). Presentation: Carrying out of Strength Tests of Geared Motor Box as Part of a Frequency-Controlled Traction Electric Drive. Sofia, Bulgaria: IEEE, 2021.
3. IEEE 62nd International Scientific Conference on Power and Electrical Engineering of Riga Technical University (RTUCON 2021). Presentation: Determination of the Level of Own Vibration of Geared Motor Boxes in Industrial Conditions. Riga, Latvia: IEEE, 2021.
4. 9th International Conference on Electrical and Electronics Engineering (ICEEE 2022). Presentation: Carrying Out of Strength Control of Mutual Loaded Traction Geared Motor Boxes as a Part of Industrial Tests. Alanya, Turkey, IEEE, 2022.
5. 8th International Youth Conference on Energy (IYCE 2022). Presentation: Determination of the strength characteristics of traction gears under shock loads. Eger, Hungary: IEEE, 2022.
6. 2nd International Conference on Electrical, Computer and Energy Technologies (ICECET 2022). Presentation: Evaluation of the Strength of Traction Geared Motor Units by Permissible Stresses and the Level of Vibration Activity. Prague, Czech Republic: IEEE, 2022.
7. 3rd International Conference on Power, Energy and Electrical Engineering (PEEE2022). Presentation: The influence of dynamic loads on the vibration level of rotating units of traction drives. Barcelona, Spain: IEEE, 2022.
8. 25th International Conference on Electrical Machines and Systems (ICEMS2022). Presentation: Verification of Strength Characteristics of Traction Geared Motor Unit on Industrial Conditions. Chiang Mai, Thailand: IEEE, 2022.
9. 25th International Conference on Electrical Machines and Systems (ICEMS2022). Presentation: Strength and Vibration Activity Control of Traction Geared Motor Units. Chiang Mai, Thailand: IEEE, 2023.

10. 10th International Conference on Electrical and Electronics Engineering (ICEEE2023). Presentation: Evaluation of Vibrational Activity of Laminated Cases of Traction Electric Machines According to Actual Condition. Istanbul, Turkey: IEEE, 2023.
11. 18th International conference on electrical machines, drives and power systems (ELMA2023). Presentation: Determination of the Level of Vibroactivity of the Traction Motor-Gear Units. Varna, Bulgaria: IEEE, 2023.
12. 36th International Conference on Electrical Drives and Power Electronics (EDPE2023). Presentation: Experimental Study on the Strength of Geared Motor Units by Using Vibration Spectrum. The High Tatras, Slovakia: IEEE, 2023.
13. 6th Global Power, Energy and Communication Conference (GPECOM2024). Presentation: The Influence of Magnetic Traction Force of Geared Motor Boxes Vibration. Hungary, Budapest: IEEE, 2024.
14. 23rd International Symposium on Electrical Apparatus and Technologies (SIELA2024). Presentation: The influence of the tension of the MGU casing on its dynamic characteristics. Bourgas, Bulgaria: IEEE, 2024.
15. Conference on Advanced Topics on Measurement and Simulation (ATOMS2024). Presentation: Effect of Magnetic Traction Force on Drive Vibration Activity. Constanta, Romania: IEEE, 2024.
16. 25th International Conference on Electromagnetics in Advanced Applications (ICEAA2024). Presentation: Impact of Magnetic Traction on Drive Vibration Dynamics. Lisboa, Portugal: IEEE, 2024.
17. 13th IEEE International Conference and Exposition on Electrical and Power Engineering (EPEi 2024). Presentation: The Influence of Bearing Bore Wear on Power Indicators of the Traction Motor-Gear Unit. Jasi, Romania: IEEE, 2024.

The results of the Thesis were presented in the following conference proceedingss.

1. Dvornikovs, I., Marinbahs, M., Kobenkins, G., Sliskis, O., Ketners, K. “Carrying out of Tests for the Functionality of the Traction Autonomous Drives in the Conditions of Industry and Serial Production.” In: *2021 17th Conference on Electrical Machines, Drives and Power Systems (ELMA 2021)*, Bulgaria, Sofia, 1–4 July 2021. Piscataway: IEEE, 2021, pp. 189–192. ISBN 978-1-6654-1186-8. e-ISBN 978-1-6654-3582-6. Available from: doi:10.1109/ELMA52514.2021.9503099.
2. Kobenkins, G., Marinbahs, M., Burenin, V., Zarembo, J., Sļiskis, O. “Carrying out of Strenght Tests of Geared Motor Box as Part of a Frequency-Controlled Traction Electric Drive.” In: *2021 17th Conference on Electrical Machines, Drives and Power Systems (ELMA 2021*), Bulgaria, Sofia, 1–4 July 2021. Piscataway: IEEE, 2021, pp. 185–188. ISBN 978-1-6654-1186-8. e-ISBN 978-1-6654-3582-6. Available from: doi:10.1109/ELMA52514.2021.9502985.
3. Kobenkins, G., Marinbahs, M., Zarembo, J., Burenin, V., Bizans, A., Sliskis, O. “Determination of the Level of Own Vibration of Geared Motor Boxes in Industrial Conditions.” In: *2021 IEEE 62nd International Scientific Conference on Power and Electrical Engineering of Riga Technical University (RTUCON 2021)*, Latvia, Riga, 15–17 November 2021. Piscataway: IEEE, 2021, ISBN 978-1-6654-3805-6. e-ISBN 978-1-6654-3804-9. Available from: doi:10.1109/RTUCON53541.2021.9711589.

4. Kobenkins, G., Marinbahs, M., Bizans, A., Rilevs, N., Burenin, V., Sliskis, O. “Carrying Out of Strength Control of Mutual Loaded Traction Geared Motor Boxes as a Part of Industrial Tests.” In: *2022 9th International Conference on Electrical and Electronics Engineering (ICEEE2022)*, Turkey, Alanya, 29–31 March 2022. Piscataway: IEEE, 2022, pp. 185–189. ISBN 978-1-6654-6755-1. e-ISBN 978-1-6654-6754-4. Available from: doi:10.1109/ICEEE55327.2022.9772530.
5. Marinbahs, M., Kobenkins, G., Pavelko, V. Bizans, A., Rilevs, N., Sliskis, O. “Determination of the Strength Characteristics of Traction Gears Under Shock Loads.” In: *The 8th International Youth Conference on Energy (IYCE2022)*, 6–9 July 2022, Eger, Hungary. Available from: doi: 10.1109/IYCE54153.2022.9857535.
6. Kobenkins, G., Marinbahs, M., Bizans, A., Rilevs, N., Burenin, V., Sliskis, O. “Evaluation of the Strength of Traction Geared Motor Units by Permissible Stresses and the Level of Vibration Activity.” In: *Proc. Of the International Conference on Electrical, Computer and Energy Technologies (ICECET2022)*, 20–22 July 2022, Prague, Czech Republic. Available from: doi: 10.1109/ICECET55527.2022.9872590.
7. Kobenkins, G., Marinbahs, M., Bizans, A., Rilevs, N., Sliskis, O. “The influence of dynamic loads on the vibration level of rotating units of traction drives.” In: *Proc. 3rd International Conference on Power, Energy and Electrical Engineering (PEEE2022)*, 18–20 November 2022, Barcelona, Spain. Available from: doi: 10.1016/j.egyr.2022.12.114.
8. Kobenkins, G., Marinbahs, M., Bizans, A., Sliskis, O. “Verification of Strength Characteristics of Traction Geared Motor Unit on Industrial Conditions.” In: *Proc. of the 25th International Conference on Electrical Machines and Systems (ICEMS2022)*. 29 November – 2 December 2022, Chiang Mai, Thailand. Available from: doi: 10.1109/ICEMS56177.2022.9982859.
9. Kobenkins, G., Marinbahs, M., Bizans, A., Sliskis, O. “Strength and Vibration Activity Control of Traction Geared Motor Units.” In: *Proc. of the 25th International Conference on Electrical Machines and Systems (ICEMS2022)*. 29 November – 2 December, Chiang Mai, Thailand. Available from: doi: 10.1109/ICEMS56177.2022.9983283.
10. Kobenkins, G., Marinbahs, M., Rilevs, N., Sliskis, O. “Evaluation of Vibrational Activity of Laminated Cases of Traction Electric Machines According to Actual Condition.” In: *Proc. of the 10th International Conference on Electrical and Electronics Engineering (ICEEE2023)*. 8–10 May, Istanbul, Turkey. Available from: doi: 10.1109/ICEEE59925.2023.00068.
11. Kobenkins, G., Marinbahs, M., Bizans, A., Rilevs, N., Sliskis, O. “Determination of the Level of Vibroactivity of the Traction Motor-Gear Units.” In: *Proc. of the 18th International conference on electrical machines, drives and power systems (ELMA2023)*. 29 June – 1 July 2023, Varna, Bulgaria. Available from: doi: 10.1109/ELMA58392.2023.10202391.
12. Kobenkins, G., Marinbahs, M., Rilevs, N., Sliskis, O. “Experimental Study on the Strength of Geared Motor Units by Using Vibration Spectrum.” In: *Proc. of the 36th International Conference on Electrical Drives and Power Electronics (EDPE2023)*. 2023, The High Tatras, Slovakia. Available from: doi: 10.1109/EDPE58625.2023.10274034.
13. Kobenkins, G., Marinbahs, M., Rilevs, N., Bizans, A., Sliskis, O. “The Influence of Magnetic Traction Force of Geared Motor Boxes Vibration.” In: *Proc. of the 6th Global Power, Energy and Communication Conference (GPECOM2024)*: 4–7 June 2024, Budapest, Hungary. Available from: doi: 10.1109/GPECOM61896.2024.10582650.

14. Kobenkins, G., Rilevs, N., Marinbahs, M., Podgornovs, A., Bizans, A., Sliskis, O. “The influence of the tension of the MGU casing on its dynamic characteristics.” In: *Proc. of the 23rd International Symposium on Electrical Apparatus and Technologies (SIELA2024)*. 12–15 June 2024, Bourgas, Bulgaria. Available from: doi: 10.1109/SIELA61056.2024.10637827.
15. Kobenkins, G., Marinbahs, M., Rilevs, N., Bizans, A., Sliskis, O. “Effect of Magnetic Traction Force on Drive Vibration Activity.” In: *Proc. of the Conference on Advanced Topics on Measurement and Simulation (ATOMS2024)*: 28–30 August 2024, Constanta, Romania.
16. Kobenkins, G., Rilevs, N., Marinbahs, M., Bizans, A., Sliskis, O. “Impact of Magnetic Traction on Drive Vibration Dynamics.” In: *Proc. of the 25th International Conference on Electromagnetics in Advanced Applications (ICEAA2024)*: 2–6 September 2024, Lisboa, Portugal.
17. Kobenkins, G., Marinbahs, M., Rilevs, N., Bizans, A., Sliskis, O. “The Influence of Bearing Bore Wear on Power Indicators of the Traction Motor-Gear Unit.” In: *Proc. of the 13th IEEE International Conference and Exposition on Electrical and Power Engineering (EPEi 2024).* 17–19 October 2024, Jasi, Romania.

CHAPTER 1. CURRENT STATE OF APPROACHES TO ASSESSING THE TECHNICAL CONDITION OF RAILWAY EQUIPMENT

As was noted during the IMECO conference, there might be a possible increase in technical use, the so-called safety factor by more than 12 %, due to the introduction of diagnostic tools and preliminary equipment control before transferring it to serial operation. In turn, the time for downtime and repair of rolling stock due to preventive control and diagnostic measures can be reduced to 40 %. In turn, the quality and completeness of diagnostic measures, as well as the set of interrelations of controlled parameters determine the reliability of diagnostic signs and accompanying phenomena.

The author of the Thesis, based on the methods of vibration diagnostics of motor gear units (hereinafter – MGU) of railway transport (see Fig. 1.1), set the task of identifying the most informative combinations of signs of major faults reflected in the frequency and time domains. In this case, the traction and energy indicators of the MGU are presented in the frequency domain of the hormonal spectrum, and the root-mean-square value of vibration is presented in the time domain [1].

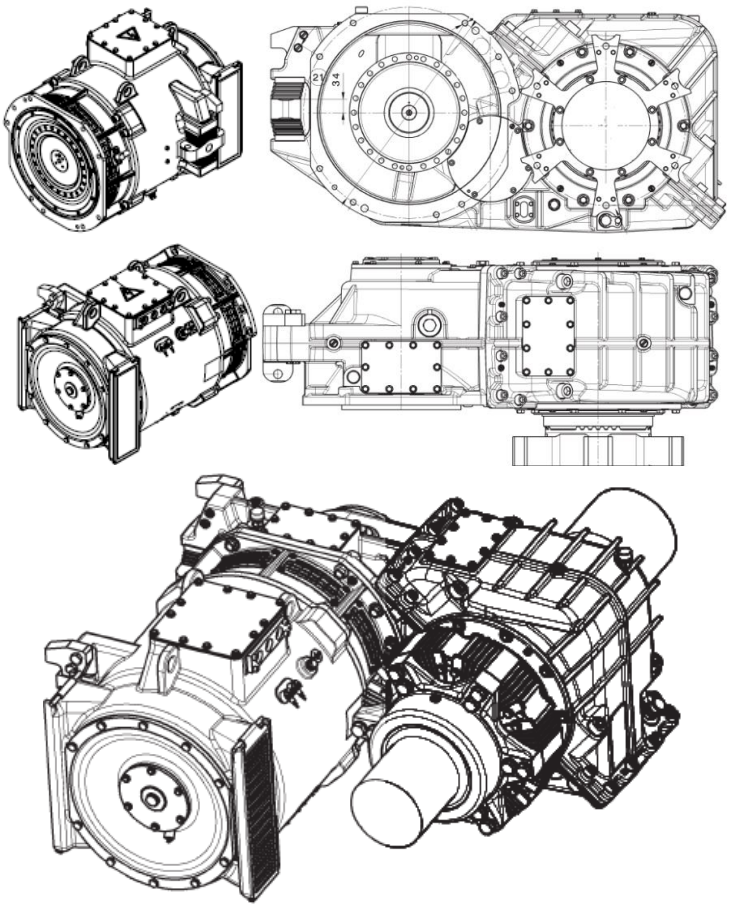

Fig. 1.1. Structure of traction MGU.

The Thesis presents in detail the understanding of torsional vibrations and their influence on dynamic processes, in particular those occurring in the air gap of the motor. The undoubted advantage of the Thesis is not only laboratory research but also experiments in real operation mode. Due to the fact that the study covers various types of traction motors, the author presented for analysis various electric traction control systems, namely voltage and frequency converters, current converters and switching loads.

1.1. Common terminology used for machinery vibration

The **velocity** of vibration is measured in peak units such as millimetres per second (mm/s). Velocity measurements and monitoring of vibration are the most common units to identify various problems or acceptability such as unbalance, misalignment, looseness (machinery structural, foundations, or bearings), harmonics, and many other issues in the machinery frequency range and many multiples of actual speed.

Acceleration is very important for the detection of faults with bearings, gear mesh or electrical issues. Acceleration is measured in acceleration units of G. Simplified – millimetres per second/second (mm/s/s). Acceleration data are relevant in the rotational axis only.

Displacement is measured in peak-to-peak units of millimetres (mm). Displacement measurements are recorded in the same three directions as velocity – axial, horizontal and vertical. Displacement is not used or recommended for recording or monitoring because severity or acceptability is speed dependent. Displacement is also used to identify problems in the lower frequency ranges.

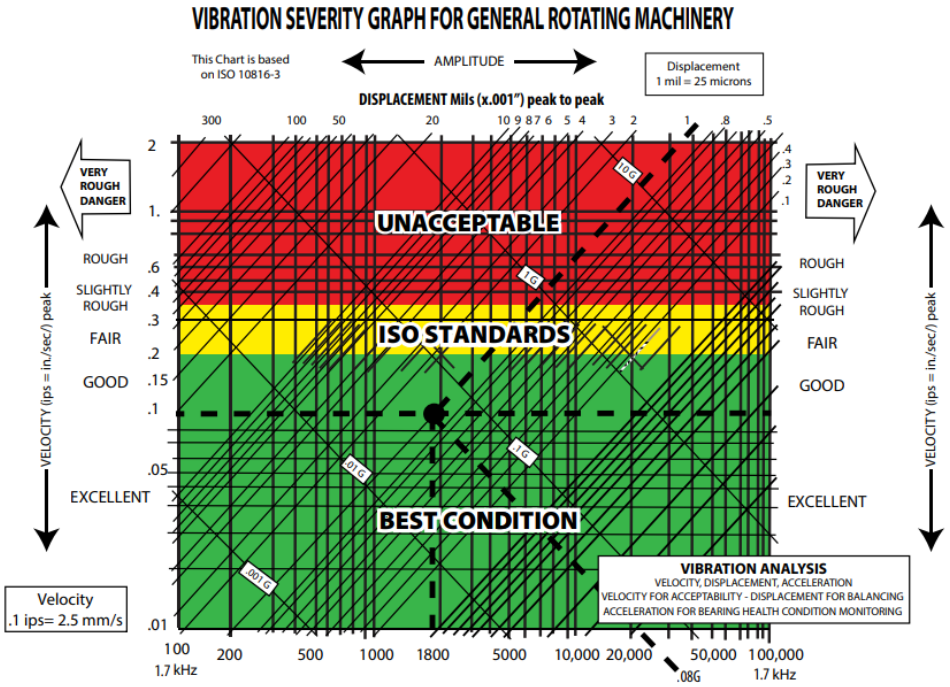

Fig. 1.2. Vibration severity graph for rotating machinery.

1.2. Mechanisms behind rail-induced vibrations

During the movement, the train creates a combined dynamic system, causing vibration excitations, primarily in the track circuit. Despite the vibration damping systems provided in the designs of the electric train bogies, such as shock absorbers, springs and cushions, the moving train remains a powerful source of vibration excitations. In turn, the smooth passage of the wheel pair along the rails is affected by their wear, laying and the condition of the embankment, which together also have some shock-absorbing properties capable of suppressing vertical vibrations [2].

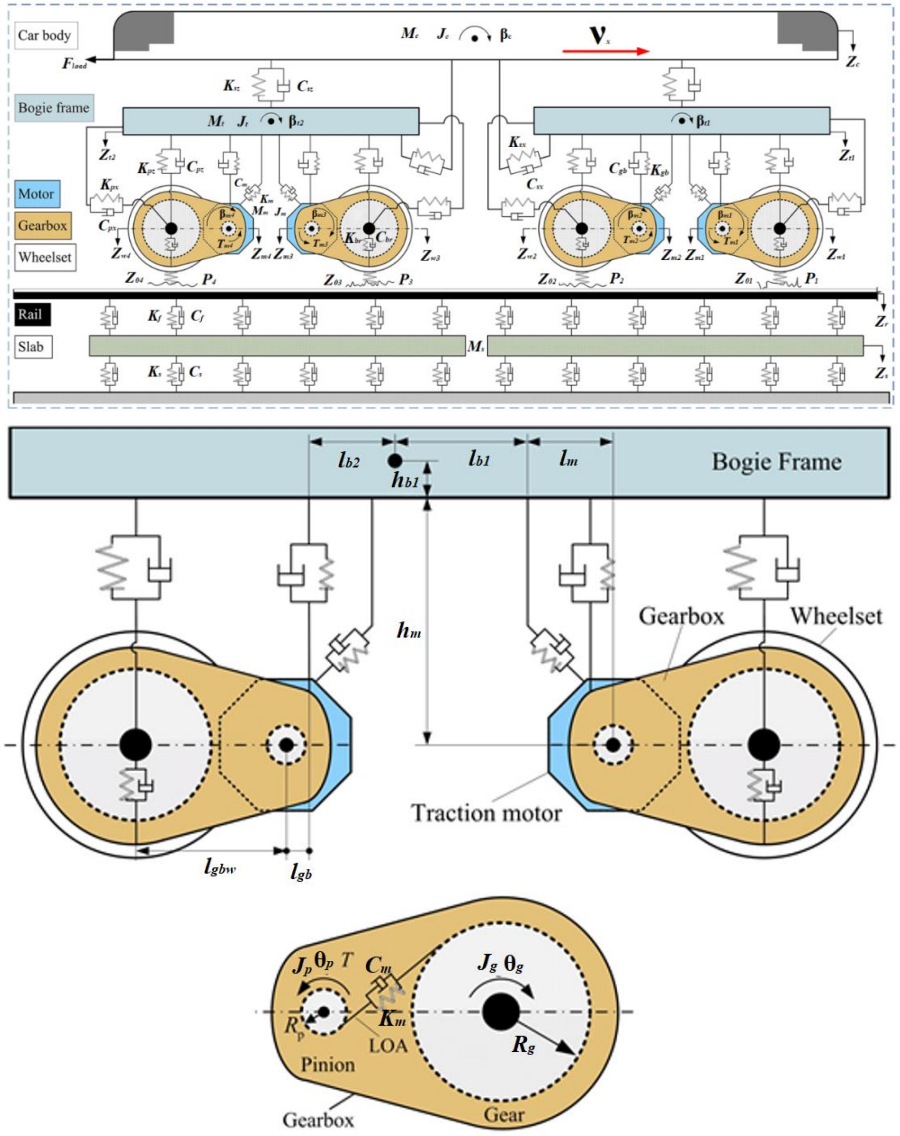

Fig. 1.3. Vehicle–track coupled dynamics model of vehicle with traction motors and gear transmissions [3].

$K_{pz}, C_{pz}, K_{px}, C_{px}$ – primary suspension refers to the steel spring and the shock absorber between the bogie frame and the axle box;

$K_{sz}, C_{sz}, K_{sx}, C_{sx}$ – secondary suspension denotes the air spring between the bogie frame and the car body;

T_{mi} – gear transmission systems in gearboxes transmit the traction torques from traction motors to wheelsets, generating longitudinal creep force at the wheel-rail contact interface.

The vibration frequencies generated by the described mechanisms are influenced by the train's speed. Table 1.1 illustrates the frequency range for each vibration source at train speeds of 40 km/h, 80 km/h, and 160 km/h. For rail, higher velocities are possible, though they are not included in this table.

Table 1.1

Approximate Frequencies of Standard Vibrations for Each of the Producing Mechanisms, Based on Train Speed (for illustrative purposes only)

Vehicle speed	**40 km/h**	**80 km/h**	**160 km/h**
Moving load (axle gap around 1.8 m)	3 Hz	5 Hz	11 Hz
Track irregularities	4 Hz 100 Hz	2 Hz 200 Hz	4 Hz 400 Hz
Rail surface wear	~ 500 Hz	~ 1000 Hz	~ 2000 Hz
Wheel surface irregularities	4 Hz	8 Hz	15 Hz
Wheel polygonal wear (with a wavelength of 0.1 m)	~ 100 Hz	~ 200 Hz	~ 400 Hz
Bogie gap (around 8 m)	~ 1 Hz	~ 3 Hz	~ 5 Hz
Sleeper gap (0.6 m)	Multitudes of 16 Hz	Multitudes of 32 Hz	Multitudes of 64 Hz

1.3. Standards and regulations

The majority of systems and equipment control frameworks rely on the following standards:

1) *ISO 13373-1-2002* – Vibration condition monitoring of machines. This guideline outlines the fundamental principles of vibration monitoring, the kinds of sensors used, and their mounting locations [4].

2) *ISO 15242-1-2015* – Vibration measurement methods. This regulation defines the vibration rating of rolling bearings and sets the criteria for environmental conditions during measurement (limited to a test bench) [5].

3) *ISO 2041:2009* – Vibration Terms and Definitions. This international standard defines the fundamental terms and concepts used in the field of vibration [6].

4) *ISO 20816-3:2022* – Mechanical vibration – Measurement and evaluation of machine vibration [7].

5) *ISO 17359:2018* – Condition monitoring and diagnostics of machines – General guidelines.

Several standards also offer main guidelines for data interpretation and machine diagnostics:

1) *ISO 13379-1:2012* – Condition monitoring and diagnostics of machines – Data interpretation and diagnostics techniques. Part 1: General guidelines [8].

2) *ISO 13379-2:2015* – Condition monitoring and diagnostics of machines – Data interpretation and diagnostics techniques. Part 2. Data-driven approach [9].

The aforementioned normative documents demonstrate the advanced development of vibration diagnostic methods.

1.4. Analytical review of motor monitoring and diagnostic methods

Data from the Institute of Electrical and Electronics Engineers (IEEE) and the Electric Power Research Institute (EPRI) show that over 40 % of all IM failures are due to bearing issues, as depicted in Fig. 1.4.

These failures are critical as they increase both vibration and noise levels in IMs [10]. The main reasons for bearing defects include material fatigue, heightened air gap eccentricity, unbalanced loads, shaft misalignment, nearby equipment vibrations, and torque fluctuations.

The main stator faults include open winding circuits and short circuits. An open circuit in the stator winding leads to an increase in the reverse sequence current amplitude, which can be detected by comparing the direct and reverse sequence current amplitudes, and when these values approach each other, the protection system is triggered.

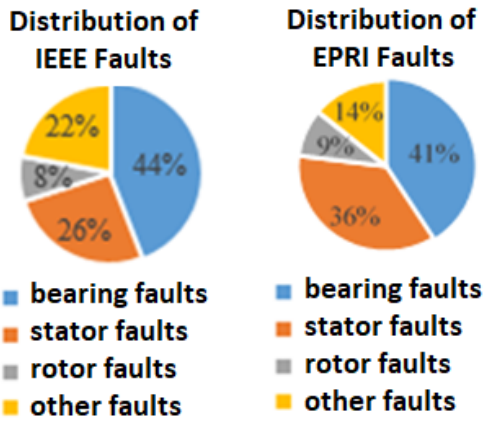

Fig 1.4. Fault distribution according to IEEE and EPRI.

1.5. Chapter conclusions

1. The analysis of various maintenance strategies suggests that continuous monitoring of the technical condition is optimal from both economic and energy perspectives.

2. The most promising approaches are those based on current and vibration measurements since the main types of faults affect these parameters. These indicators are also convenient for monitoring; in particular, current diagnostics can be easily integrated into existing motor protection systems since it already involves measuring the current in the stator windings. The main disadvantages of current methods include:

- requirement for long-term signal sampling;
- high computational complexity;
- need for prior knowledge of motor slip.

CHAPTER 2. EFFECT OF TRACTION TRANSMISSION ON THE DYNAMICS OF ELECTRIC TRAINS

2.1. Impact of the electrical component of traction transmission on dynamic characteristics of railway vehicles

The power supply system of the train can be represented by various configurations of power and actuator mechanisms, the role of which is performed by traction MGU in the train. For MGU with asynchronous traction motors, the power source is a traction converter – a source of alternating non-sinusoidal current [11]. Further, MGUs located on motor bogies can be connected individually or in pairs to the power outputs of the traction converter. The train layout can include purely motor cars, but another option is also possible with the installation of a motor bogie on each car. Recently, preference has been given to the second option. Usually, the power part of the converter includes an adjustable DC link, a block of traction inverters, the function of which is to regulate the voltage and frequency level, and directly the inverter control system, often implemented on IGBT transistor modules [12], [13]. In addition, the converter is equipped with a processing unit for feedback signals, motors, braking systems, etc., which makes it possible to regulate the torque and speed of the motor rotor.

2.1.1. General approach to the development of a mathematical model of traction transmission. Analytical representation of transmission system

The interaction between the 11th and 13th harmonics and the main magnetic field creates the 12th harmonic torque. In the simplified gear transmission system, pure torsional vibration is considered.

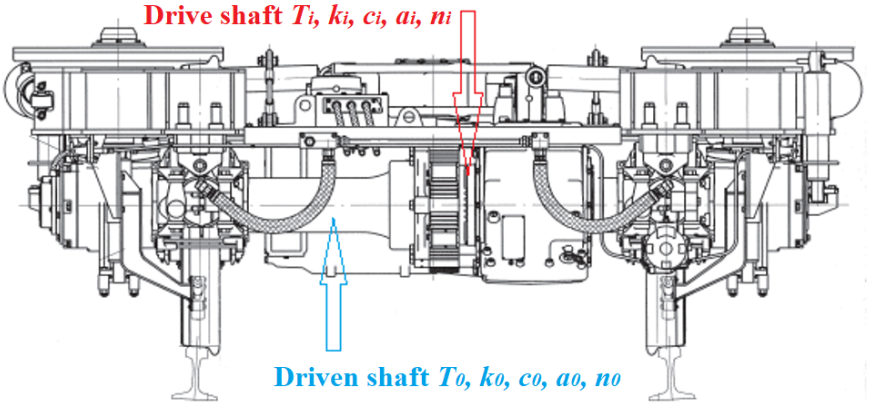

J – equivalent rotational inertia of the entire transmission system as referred to the wheel axle; J_1 – inertia of the left wheel; J_2 – inertia of the right wheel; k_1 – the equivalent torsion stiffness between the transmission system and the wheel–set; k_2 – torsion stiffness of wheel–set; c_1 – equivalent torsion damping between the transmission system and the wheel–set; c_2 – torsion damping of wheel–set; T_e – electromagnetic torque generated by the traction motor; T_1 – opposing torque exerted by the rail to the left wheel; T_2 – opposing torque exerted by the rail to the right wheel; θ_1 – torsion angle displacement between the traction motor and the left wheel; θ_2 – torsion angle displacement between the left and right wheels.

Fig. 2.1. Gearbox built in bogie and a schematic representation of the torsional vibration.

Here, k_i and k_0 represent the torsional stiffness of the drive and driven shafts, respectively; c_i and c_0 represent their torsional damping coefficients; α_i and α_0 are the angular displacements; and n_i and n_0 are their angular velocities (Fig. 2.1). The driving torque is denoted as T_i and T_0, where the gear ratio is specified as:

$$N = \frac{n_i}{n_0}. \tag{2.1}$$

The dynamic equation for gear transmission torque is:

$$T = k(\alpha_0 - \frac{\alpha_i}{N}). \tag{2.2}$$

It can be assumed that for the right and left wheels of the motor sled the value of rotational inertia will have an equal value, and then the system of equations of torsional vibrations will take the following form:

$$\begin{bmatrix} J_1 & 0 \\ 0 & J_2 \end{bmatrix}\begin{bmatrix} \ddot{\theta}_1 \\ \ddot{\theta}_2 \end{bmatrix} + \begin{bmatrix} c & -c_2 \\ -c_1 & 2c_2 \end{bmatrix}\begin{bmatrix} \dot{\theta}_1 \\ \dot{\theta}_2 \end{bmatrix} + \begin{bmatrix} k & -k_2 \\ -k_1 & 2k_2 \end{bmatrix}\begin{bmatrix} \ddot{\theta}_1 \\ \ddot{\theta}_2 \end{bmatrix} = \begin{bmatrix} -\frac{J_1}{J}T_e - T_1 \\ T_1 - T_2 \end{bmatrix}. \tag{2.3}$$

2.2. Analysis of vibration studies of traction drive system components based on field tests of electric trains

2.2.1. Vibration properties of traction motor

To dampen torque pulsations in AC-DC-AC traction drive systems, two methods are used: software and hardware using DC components in the DC link [14], [15]. In case of imperfect calculations, or as a result of incorrect selection of filter components, this method may not be effective, in which case the pulsating torque of the motor will increase and already, to a greater extent, will affect the fatigue damage of the suspension and fasteners of the MGU. The MGU is located on the motor frame and is fixed in places, as shown in Fig. 2.2.

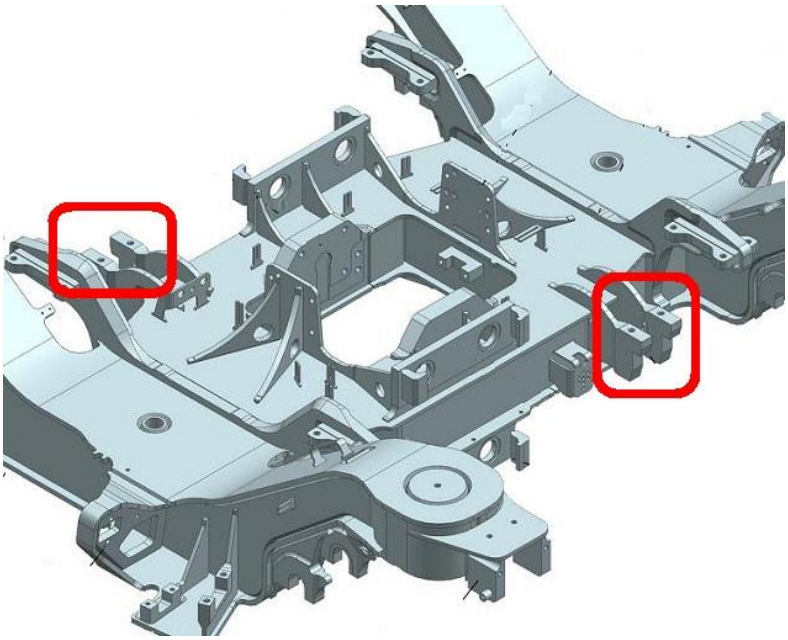

Fig. 2.2. Configuration of the traction motor suspension system.

Due to the fastening of the supporting MGU elements by welding to the bogie frame, fatigue processes in these connections occur even faster, especially under the influence of vibration and with a worn-out shock absorption system of cars. In addition to the above, among the external sources of vibration disturbances, the most obvious are excitations transmitted from the "rail-wheel" contact [15].

2.2.2. Vibration characteristics of gearbox

The MGU is designed to transmit torque from the motor to the wheel of the motor bogie. Usually, in suburban and regional electric trains, the motor bogie contains two-wheel pairs and, accordingly, two MGUs. Inside the MGU, the motor rotor is connected to the input shaft of the gearbox (from the small gear side) by insulated elastic half-couplings, which are the first step in damping vibrations from the drive side, then the system of gears and bearings, the output hollow shaft of the gearbox is connected by means of a wedge-packet clutch to the axle of the wheel pair, which is another step in damping torsional vibrations. Unlike the case of rigid coupling of the axle of the wheel pair with the input shaft of the gearbox, in the case described, the suspension and shock absorption system of the MGU itself is simplified [16], [17].

2.3. Dynamics of electric machines

The main contributor to electromagnetic vibration noise in motors is the radial electromagnetic force created by the magnetic field in the air gap. In studies of electromagnetic force excitation, most research focuses on radial force excitation under ideal sinusoidal current inputs. Traditional electromagnetic noise models tend to focus mainly on radial forces, often overlooking other components of electromagnetic force, which can reduce the precision of simulations. Tangential electromagnetic forces affect electromagnetic noise, and models that include all three components – radial, tangential, and axial forces – offer a more accurate and dependable representation.

The results, examined via frequency response analysis [18], revealed that tangential forces induce considerably greater tangential deformation in the stator teeth than radial forces. In the frequency spectrum, the second-order torque ripple frequency, closely tied to tangential electromagnetic forces, has a significant impact on electromagnetic vibration.

2.3.1. Dynamics of electric machines in the context of magnetic attraction

Mechanical oscillations in electrical machines are distinct due to the presence of a fluctuating magnetic field. If there is an uneven air gap between the rotor and stator, which can be caused by static or dynamic eccentricity of the rotor, the electromagnetic field generates a radial force acting on the rotor’s centre, directed towards the region with the smallest air gap. This force is referred to as unbalanced magnetic pull (UMP).

UMP serves as a source of forced vibrations in hydro-generators and induction motors. In traction motors, the pronounced effect of electromagnetic forces on rotor oscillations is linked to both the multi-pole structure and the relatively narrow radial air gap between the rotor and stator.

2.3.2. Unbalanced magnetic pull forces in axial inductor machines

Electromagnetic attraction forces that develop in electrical machines are due to the change in magnetic energy stored within the air gap as a function of the moving part's displacement. In rotating machinery, the tangential components of these forces produce electromagnetic torque, while the radial components generate forces acting perpendicular to the rotor's axis. However,

when this transverse magnetic symmetry is disrupted, UMP forces emerge. These forces lead to increased shaft deflection, the creation and amplification of alternating radial loads on the shaft, and heightened bearing pressure, all of which must be accounted for in the machine's design.

2.3.3. Mathematical representation of an induction motor in a multiphase coordinate system with rotor circuit asymmetry

To develop an $n-phase$ mathematical model, commonly accepted principles and formulas from the simulation of induction motors were utilized [19].

The system of differential equations for an $n-phase$ machine is expressed as:

$$\begin{cases} \frac{d\psi_s^{(1)}}{dt} = U^{(1)} - R_s \times i_s^{(1)}; \\ \cdots \\ \frac{d\psi_s^{(n)}}{dt} = U^{(n)} - R_s \times i_s^{(n)}; \\ \frac{d\psi_R^{(1)}}{dt} = 0 - R_R \times i_R^{(1)}; \\ \cdots \\ \frac{d\psi_R^{(n)}}{dt} = 0 - R_R \times i_R^{(n)}, \end{cases} \quad (2.5)$$

where R_s, R_R – stator and rotor resistance;

i_s, i_R – stator and rotor current;

ψ_s, ψ_R – stator and rotor flux linkage;

U – input voltage to the stator winding.

From the above system of Equation (2.5), it is clear that the variable determines the number of cores. As the number of rotor cores increases, the complexity of the system also grows.

The developed mathematical model is intended for studying an induction motor with a squirrel-cage winding when rotor cores are broken. The input voltage vector is composed of components from both the stator and rotor, but since the motor has a squirrel-cage winding, the input effects on the rotor circuit will always be zero [20].

2.4. Design and technological model of the air gap in the asynchronous motor

The design of the MGU is such that, due to the single-support device of the traction motor, the second end of the rotor is attached to the input shaft of the gearbox through an insulated coupling, due to which the requirements for the accuracy of the stator core (inner diameter) are extremely strict [21]. In such a design, the air gap is the most vulnerable point, and its unevenness negatively affects the energy parameters of the machine. The effect of the eccentricity of the rotor axis relative to the stator axis of the motor can be described by the expression:

$$\varepsilon_{max} = \frac{\varepsilon_{max}}{\gamma_{min}} \times 100\%, \quad (2.6)$$

where ε_{max} is maximum eccentricity of the rotor core axis relative to the stator bore axis, mm.

The presence of an uneven air gap between the stator and the rotor of the motor, in addition to reducing the efficiency of the asynchronous motor, can significantly increase the unbalanced magnetic force acting on the rotor, which can be multiple compared to the calculated values. At the same time, the service life of the bearings is reduced, and in the worst case, when the shaft axis is shifted, direct contact between the rotor and the stator can occur. The rotor

eccentricity is a significant factor that also affects magnetic noise. With an increase in misalignment from 0.05° to 0.5°, the equivalent load can increase by 2.6–2.9 times.

To create a mathematical model, the following expression is proposed:

$$\gamma_{din} = \gamma - e_{st}\cos\varphi - z_0 \times cos[48EJ(l^3 mp\omega^2)^{-1}\varphi]^{\frac{1}{2}}, \quad (2.7)$$

where

- φ, z_0 – generalized coordinates representing the rotor's rotation angle (degrees) and the dynamic eccentricity of the rotor axis relative to the stator (mm), respectively;
- E – modulus of elasticity of the rotor shaft material (kg/mm²);
- J – moment of inertia of the rotor (mm⁴);
- l – distance between rotor supports (mm);
- mp – rotor's mass (kg);
- ω – rotational frequency of the rotor (s^{-1});
- e_{st} – eccentricity of the rotor's axis relative to the stator hole (static eccentricity).

An analysis of the factors contributing to the overall air gap error shows that the greatest impact comes from the static eccentricity of the rotor ($\Delta\gamma_e = 56$ %). This is followed by errors in the stator and rotor ($\Delta\gamma_n = 35$ %), and design-operational factors ($\Delta\gamma_{keq} = 9$ %).

2.5. Chapter conclusions

1. Harmonic vibrations, especially due to non-sinusoidal AC inputs, directly affect the motor and drive systems, influencing speed variations and vibrations throughout the vehicle.

2. Non-sinusoidal currents introduced by inverters lead to harmonic distortions, which in turn cause pulsating torques. These torques impact the overall stability of the train, increasing mechanical vibrations that propagate through the drive system.

3. Direct torque control systems, along with vibration analysis models, help mitigate the adverse effects of electrical harmonics and mechanical vibrations. These systems are essential for maintaining the performance and longevity of the traction drive components.

4. In electrical machines, particularly with narrow air gaps, UMP forces significantly influence rotor dynamics, contributing to mechanical oscillations and vibrations. These forces must be accounted for in the design of rotor systems to prevent mechanical failures.

CHAPTER 3. ANALYSIS OF WEAR IN TRACTION GEAR SYSTEMS OF ELECTRIC RAIL TRANSPORT

The main tasks that need to be implemented at the design and testing stage of the rolling stock traction equipment kit are:

1. Perform the main function of the drive – provide traction, i.e., convert and transmit energy from the source to the drive (executive) mechanism. Here, it is necessary to consider both a wide operating range of torque and operating speeds, and among the operating modes, it is necessary to highlight the most critical ones – starting the movement and breaking the train.

2. Damp vibrations and prevent the possible influence of high-frequency regulation on the vibration state of the driven object, in particular the MGU.

3. Ensure reliable and safe operation of electric rolling stock in a wide climatic range.

Here it should be noted that the traction drive itself is a strong source of heat generation, which in some cases, such as disconnecting the drive after a long period of operation during the overnight period of standing, can cause the formation of condensate inside the motor with subsequent insulation flashover when it is turned on [22], [23].

Of course, when designing the traction drive of an electric train, in addition to the main traction-energy rating, i.e., when all the provided units and mechanisms operate without disconnection, an allowance is made for semi-emergency and emergency modes, when the train can move to the repair site without disembarking passengers, or to the nearest parking place for disembarking passengers.

The traction drive of an electric train is mainly subjected to the load created by the traction torque.

When the EMU moves over uneven support surfaces, the torque on its drive wheels will be different, even on a straight horizontal section. This applies even more to curved sections of the support surface. But when analyzing the traction and speed properties of the EMU, it is customary to consider them for rectilinear motion, without considering the unevenness of the support surface and the difference in radii between the wheels of the same axle. In the absence of external slip of the drive wheels, the number of drive axles (wheel pairs) is of no fundamental importance for the model built on the above assumptions. When determining the total traction torque of the drive wheels, it is necessary to consider all the components of the resistance overcome by the motor in the process of transmitting energy to the drive wheels, as well as the dissipation of energy in the transmission mechanisms. In the transmission, this torque is converted by reduction elements (gear transmissions). The conversion of torque is accompanied by losses, which are considered by means of the efficiency of the mechanical transmission. At the same time, part of the transmitted energy of the electric motor is spent on accelerating the rotating masses (parts) of the transmission, which are also connected to the drive wheels. Therefore, when overcoming the resistance to the acceleration of the transmission masses, it is necessary to consider the efficiency of the reduction gear elements.

The motion mode of the EMU is determined by the ratio of all forces and moments acting on it. An analysis of all forces acting on the EMU during its motion shows that under normal operating conditions, three motion modes are possible: traction, coasting and braking.

3.1. Dynamics and durability of electric train traction drives

For each type of electric train, which is designed for a specific railway network and schedule, there is a loading cyclogram that takes into account the distances on the platforms between stations, the speed of movement on the platforms taking into account the load on the branch, as well as the required time for the train to be in the main operating modes – starting, moving at nominal speed, coasting, braking and stopping.

The main calculated values required for performing traction-energy calculations are the motor power on the shaft, the traction force on the wheel rim when starting off, the continuous traction force on the stretches, as well as the value of the maximum traction force, taking into account the adhesion limitation.

The force in the gear mesh and the vertical reaction in the gear bearings can be calculated based on the transmission geometry (see Fig. 3.1):

$$P_1 = \frac{D_w F}{D_{gw}}, \tag{3.1}$$

where D_w is the diameter of the wheel band around the riding circle; and D_{gw} is the diameter of the large gear wheel at the base circle.

The longitudinal forces in the gearbox suspension yoke are determined as:

$$P = \frac{P_1}{\cos\alpha}, \tag{3.2}$$

where $\alpha = 15°$, $\cos\alpha = 0.966$.

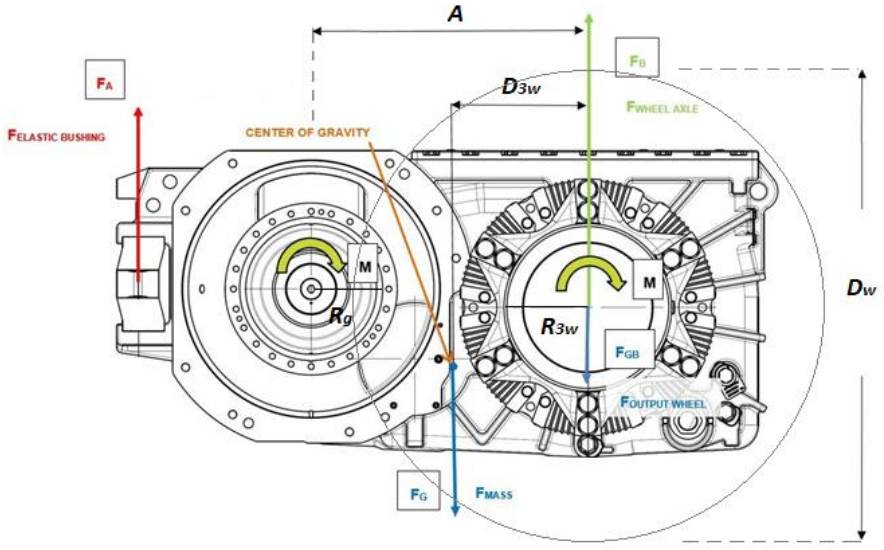

Fig 3.1. Geometric dimensions of the traction drive.

As the wheelset moves over track irregularities (see Fig. 3.2), point of the gearbox, along with the wheelset, experiences vertical acceleration . In this case, the acceleration of the centre of gravity is determined as in [24]:

$$\ddot{Z}_c = \frac{\ddot{Z}_k a_c}{A}. \tag{3.3}$$

The inertia force of the gearbox housing generates an additional load on the gearbox suspension, calculated as:

$$P_{1din} = \frac{M_k \ddot{Z}_c (A - a_c)}{A} = \frac{M_k \ddot{Z}_k a_c (A - a_c)}{A^2} = \frac{M_k \ddot{Z}_k a_c a_c'}{A^2}. \quad (3.4)$$

where M_k is the mass of the gearbox housing, including the pinion and half-coupling.

The rotational acceleration of the gearbox casing $\ddot{\varphi} = \frac{\ddot{Z}_k}{A}$ due to inertia reduces the load on the suspension by the amount:

$$P_{din} = \frac{I_c \ddot{\varphi}}{A} = \frac{I_c \ddot{Z}_k}{A^2}, \quad (3.5)$$

where I_c is a moment of inertia of the gearbox casing, inclusive of the pinion and half-coupling, relative to its centre of mass.

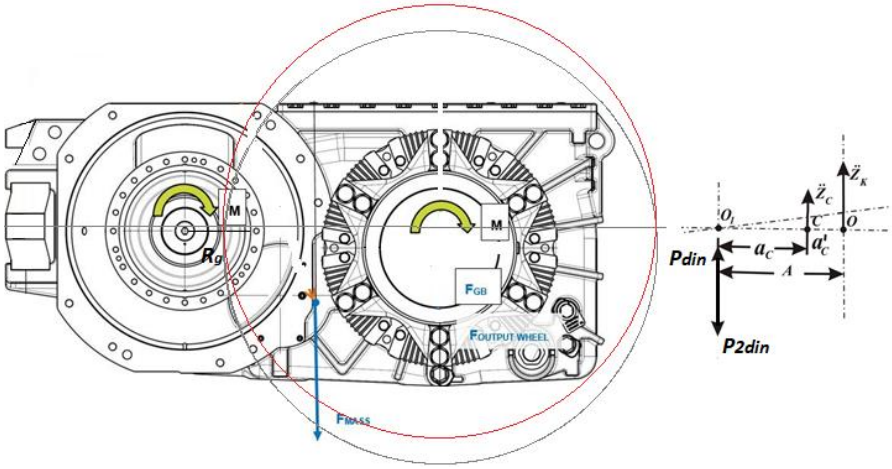

Fig. 3.2. Schematic of the forces affecting the traction gearbox when passing track irregularities.

3.2. Torsional-rotational vibrations in single-mass and two-mass systems

For the purpose of analyzing torsional and rotational vibrations, most machine assemblies can be simplified into a two-mass model. In this model, the concentrated masses typically represent the rotor masses of the machine – specifically, the rotor of the motor and the rotor of the driven machine [25]. The masses of the transmission elements are reduced to these concentrated masses.

The differential equations that describe the vibrations of this system are:

$$\theta_1 \ddot{\varphi}_1 + b_\varphi (\dot{\varphi}_1 - \dot{\varphi}_2) + C_\varphi (\varphi_1 - \varphi_2) = M_1(\omega); \quad (3.6)$$

$$\theta_2 \ddot{\varphi}_2 + b_\varphi (\dot{\varphi}_2 - \dot{\varphi}_1) + C_\varphi (\varphi_2 - \varphi_1) = M_2(t), \quad (3.7)$$

where θ_1 and θ_2 – moments of inertia associated with the rotors of the electric motor and the working machine, respectively;

C_φ and b_φ – equivalent stiffness and damping coefficients of the transmission system;

$M_1(\omega)$ – torque produced by the motor, which depends on its rotational speed;

$M_2(t)$ – torque due to resistance forces, which is a function of time.

The solutions to Equations (3.6) and (3.7) can be expressed as $\varphi_1 = \varphi_{11} \cos \omega t + \varphi_{12} \sin \omega t$ and $\varphi_1 = \varphi_{21} \cos \omega t + \varphi_{22} \sin \omega t$.

The amplitudes of the angular displacements for masses θ_1 and θ_2 are calculated by (3.8):

$$\varphi_{1a} = \sqrt{\varphi_{11}^2 + \varphi_{12}^2};\ \varphi_{2a} = \sqrt{\varphi_{21}^2 + \varphi_{22}^2}. \quad (3.8)$$

However, when analyzing transmission mechanisms, it is often more crucial to determine the amplitudes and phases of the relative rotational vibrations between the masses θ_1 and θ_2.

To simplify the equations, divide Equation (3.6) by θ_1, and Equation (3.7) by θ_2. Subtracting the second equation from the first and defining the relative angular displacement as:

$$\varphi_{12} = \varphi_1 - \varphi_2. \quad (3.9)$$

This reduction simplifies the system of Equations (3.6) and (3.7) into a single differential equation that describes the relative rotational oscillations between the two masses: θ_1 and θ_2.

$$\ddot{\varphi}_{12} + \frac{в_\varphi}{\theta_{eq}}\dot{\varphi}_{12} + \frac{C_\varphi}{\theta_{eq}}\varphi_{12} = m_1(\omega) - m_2(t), \quad (3.10)$$

where θ_{eq} is equivalent moment of inertia of the masses, given by:

$$\theta_{eq} = \frac{\theta_1\theta_2}{\theta_1+\theta_2};\ m_1(\omega) = \frac{M_1(\omega)}{\theta_1};\ m_1(\omega) = \frac{M_2(t)}{\theta_2}. \quad (3.11)$$

Assuming that $\frac{b_\varphi}{\theta_{eq}} = 2\varepsilon_\varphi;\ \frac{C_\varphi}{\theta_{eq}} = \omega_{0\varphi}^2$ where ε_φ and $\omega_{0\varphi}$ is the damping coefficient and the natural frequency of the rotational oscillations of the masses.

In free vibration scenarios within a two-mass system, the masses rotate in opposite directions by angles inversely proportional to their moments of inertia: $\varphi_1/\varphi_2 = \theta_2/\theta_1$.

3.3. Operation of the gearbox as part of the traction drive

For prototyping and reproducing the operation of the power unit in the laboratory software for the purpose of further testing the manufactured units of equipment, a model of the input was created in the MATLAB Simulink software, Fig. 3.3.

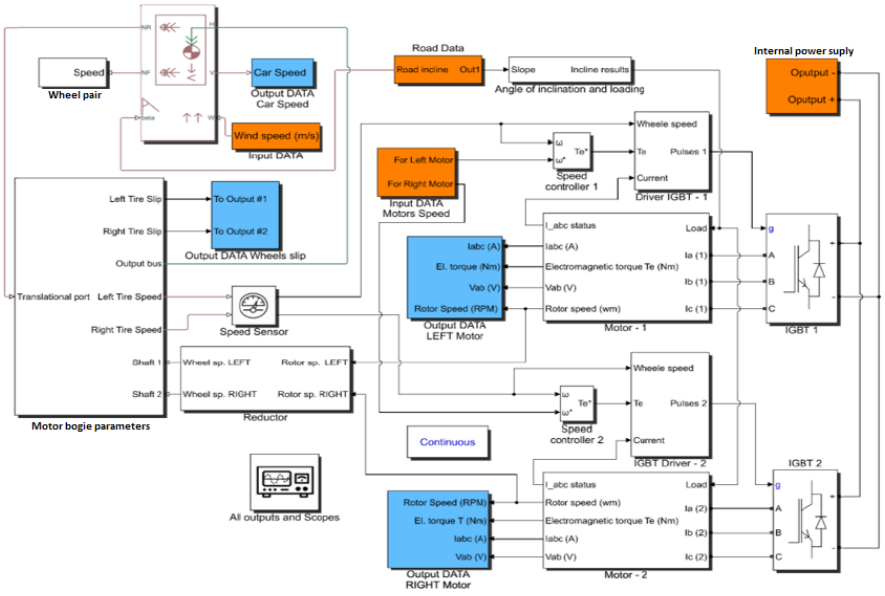

Fig. 3.3. Model of the studied traction system and parameter identification implemented in MATLAB Simulink.

This method of constructing a test bench implies alternate mutual loading of two MGUs according to the principle of "mutual loading of a two-machine “motor-generator” system" with control from a traction converter and a rheostat-brake unit. The motor and generator functions are performed by the motors equipped with gear units. The output shafts of the MGU are rigidly coupled to each other.

The speed controller VR, having received the control signal U_{input}, transmits it to the current controller IR through the current limitation and cutoff unit IMAX. The voltage controller UR receives the reference signal from IR, and the output signal is fed to the IGBT inverter [26], [27], [28]. The same IGBT inverter supplies the loaded motor. The loading motor, in turn, has feedback on the EMF (presented in Figs. 3.4, 3.5, and 3.6).

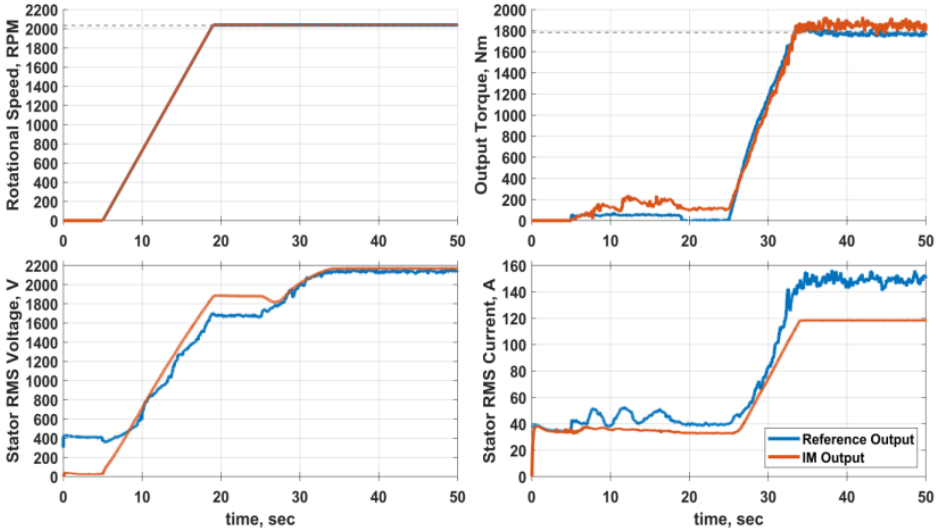

Fig. 3.4. Characteristics of the MGU during the transient process upon reaching the nominal load.

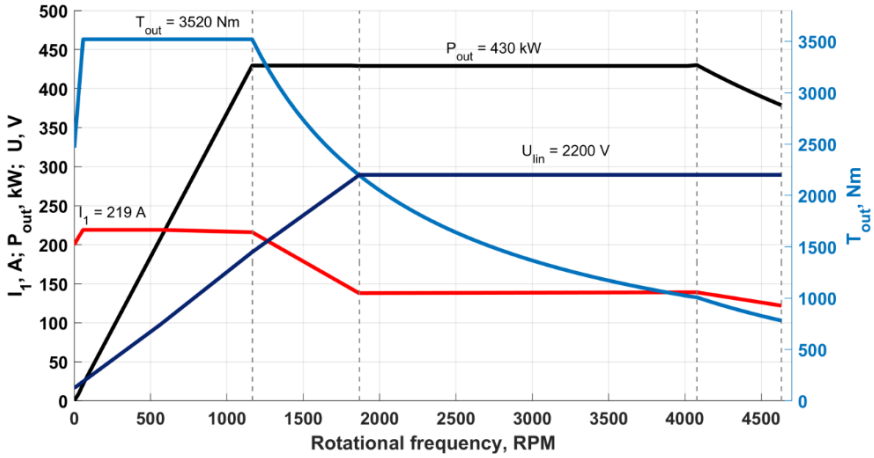

Fig 3.5. Traction diagram of EMU.

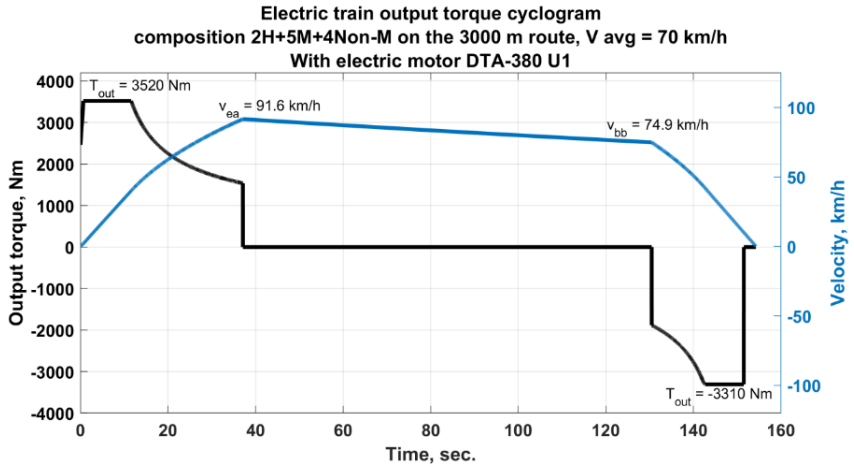

Fig. 3.6. Output torque cyclogram of EMU.

3.4. Calculation of the strength of the MGU housing

Taking into account the manufacturing technology of the MGU, it is necessary to highlight that it involves several types of preparation and processing of the materials used, so the motor and gearbox housings are made of steel or high-grade cast iron with subsequent heat treatment and tempering. The stator core is a pressed charge-welded structure. Each element has its own points of concentration of mechanical stresses, usually in places with a sharp change in the cross-section. Stress can also accumulate in places with potholes, chips, and as a result of long-term operation, also in places of wear. The most applied method that has proven itself in the mechanical engineering industry has become the finite element method (FEM), the possibility of using, which is implemented in all major automatic design systems, not to mention specialized field solvers [29], [30].

To determine the safety margin and identify the most vulnerable places in terms of mechanical stress, the critical state of which can be significantly aggravated under dynamic loads and changing vibration levels, it is necessary to have an idea of the behaviour of the object, in the specific case of the MGU, under stress-strain conditions.

The model uses the following coordinate system:

- tangential force $F_t(N)$: X-axis;
- axial force $F_r(N)$: Y-axis;
- radial force $F_x(N)$: Z-axis.

The structural material is defined as ductile iron grade EN-GJS-350-22-LT with the following strength parameters:

- modulus of elasticity E = 169 000 MPa;
- poisson's ratio μ = 0.275;
- yield strength σ_y = 220 MPa.

3.4.1. Initial calculation of bearing loads

In order to verify the appropriateness of the selected bearings, a calculation was performed to assess the accuracy of their choice according to DIN 3990:1987 standards. The input parameters for the calculations of both the first and second stages are shown in Fig. 3.7.

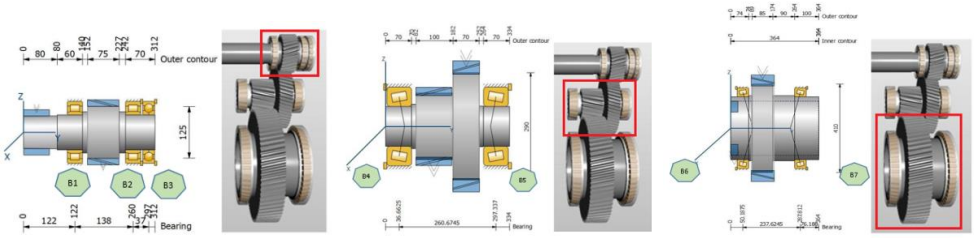

Fig. 3.7. Bearings scheme. a) input shaft; b) jack shaft; c) output shaft.

In Fig. 3.8, it is shown that at the point of suspension attachment represented by a rubber-cord shock absorber, the rotational limitation is fixed. Rotational limits are also applied at the locations of bearings. The forces created by the acceleration of the rotor mass are transmitted through the reaction forces in the bearings. The forces created by the engagement of the gears create reaction forces in the bearings. The reactions of the supports are determined from the equilibrium equation: the sum of the moments of the external forces relative to the support in question and the moment of reaction in the other support is equal to zero.

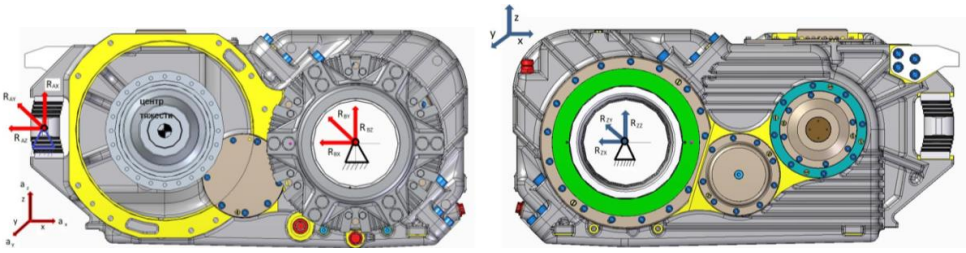

Fig. 3.8. Mounting configuration for design Modes I, II and III.
Stiffness: horizontal – 1000 N/mm; vertical – 35 000 N/mm; axial – 1900 N/mm.

3.4.2. Mode I (forward rotation)

In Mode I, the calculation is performed for the maximum motor torque during startup from a stationary position, which is 2 702 Nm. The torque is transmitted to the gear in the form of forces as follows:

- tangential force $F_t = 2M_{rot}/D_0 = 39\ 004$ N;
- radial force $F_r = F_t \cdot \mathrm{tg}\alpha / \cos\beta = 14\ 570$ N, where $\alpha = 20$ °, $\beta = 13$°;
- axial force $F_a = F_t \cdot \mathrm{tg}\beta = 9\ 005$ N, where $\beta = 13$°.

Fig. 3.9 illustrates a schematic of the bearings in the first gear stage.

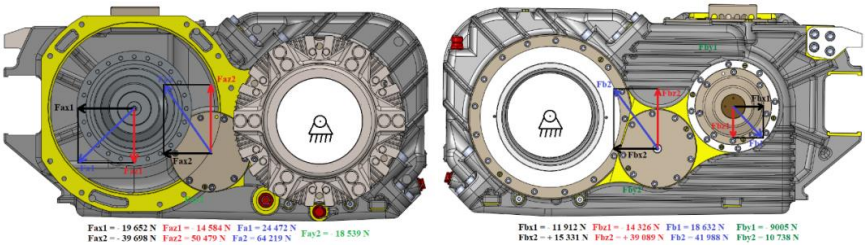

Fig. 3.9. Loads on the 1st, 2nd, 3rd, 4th and 5th bearings in operating Mode I.

3.4.3. Mode I (reverse rotation)

In reverse rotation, the combined force acting on the housing at the first bearing seat of the

operating gear within the x-z plane is spread across a 60° load angle. Additionally, there is an axial load applied to the gearbox housing at the bearing seat, as depicted in Fig. 3.10.

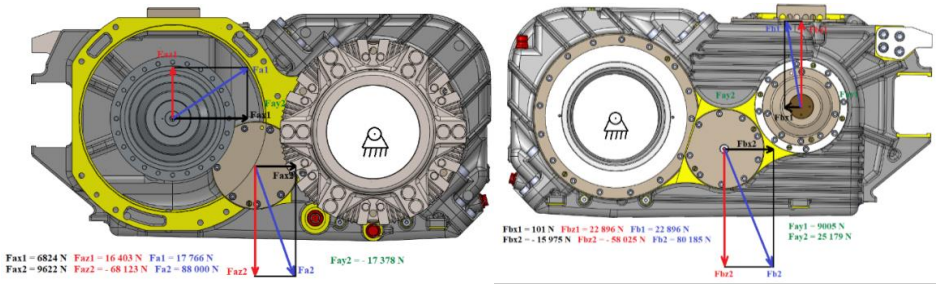

Fig. 3.10. Loads on the 1st, 2nd, 3rd, 4th and 5th bearings in operating Mode I.

3.4.4. Mode II (forward rotation)

Mode II calculations are based on the maximum starting torque of 11 000 Nm. This torque is transferred to the gear through various forces:

- tangential force $F_t = 2M_{rot}/D_0 = 158\ 845$ N;
- radial force $F_r = F_t \cdot \text{tg}\alpha / \cos\beta = 59\ 336$ N, where $\alpha = 20°$, $\beta = 13°$;
- axial force $F_a = F_t \cdot \text{tg}\beta = 36\ 672$ N, where $\beta = 13°$.

The load values for the bearings in the first stage are displayed in Table 3.1, while Table 3.2 contains the load values for the bearings in the second stage.

Table 3.1

Bearing Load Values in the First Gear Stage Based on the Coordinate System

Bearing	Force [N]						
	x´		*y´*	*z´*		*xz´*	
Direction	Forward	Reverse	Forward / reverse	Forward	Reverse	Forward	Reverse
P1	–82 075	30 467	0	–50 593	74 258	96 415	80 265
P2	–46 424	–2277	0	–61 706	91 127	77 219	91 155
P3	0	0	–36 659 / 36 659	0	0	0	0

Table 3.2

Bearing Load Values in the Second Gear Stage Based on the Coordinate System

Bearing	Force [N]						
	x´		*y´*	*z´*		*xz´*	
Direction	Forward	Reverse	Forward / reverse	Forward	Reverse	Forward	Reverse
P4	–161 508	39 460	–80 084/–78 772	205 536	–279 230	261 461	282 004
P5	82 409	– 65 324	48 328/110 529	161 365	–232 071	173 013	241 089

3.4.5. Mode III (forward rotation)

Mode III is calculated for a motor torque of up to 1 211 Nm and includes impact forces. The magnitude of the forces generated in the gearing is as follows:

- tangential force $F_t = 2M_{rot}/D_0 = 17\ 487$ N;
- radial force $F_r = F_t \cdot \text{tg}\alpha / \cos\beta = 6\ 532$ N, where $\alpha = 20°$, $\beta = 13°$;

- axial force $F_a = F_t \cdot \text{tg}\beta = 4\,037$ N, where $\beta = 13°$.

Additionally, Mode III includes impacts in all coordinate directions:

$a_x = \pm 2.5$ g (impact in the longitudinal direction);

$a_y = \pm 4.7$ g (impact in the axial direction);

$a_z = \pm 5.4$ g (impact in the vertical direction).

Tables 3.3 and 3.4 present the load values on the bearings of the first and second stages in the coordinate system.

Table 3.3

Bearing Load Values in the First Gear Stage Based on the Coordinate System

Bearing	Force [H]						
	x´		*y´*	*z´*		*xz´*	
Direction	Forward	Reverse	Forward / reverse	Forward	Reverse	Forward	Reverse
P1	2 904	–8 847	0	5 963	–7 967	6 623	11 906
P2	200	–5 299	0	10 691	–5 980	10 692	7 975
P3	0	0	4036/–4036	0	0	0	0

Table 3.4

Bearing Load Values in the Second Gear Stage Based on the Coordinate System

Bearing	Force [H]						
	x´		*y´*	*z´*		*xz´*	
Direction	Forward	Reverse	Forward / reverse	Forward	Reverse	Forward	Reverse
P4	4 337	–17 825	–7 796/–8 205	–30 759	22 444	31 063	28 661
P5	–7 184	6 905	11 292/4 709	–28 186	17 293	27 154	18 621

3.5. Chapter conclusions

This chapter presents a comprehensive analysis of wear in traction gear systems of electric rail transport. The research is focused on the operational conditions, dynamics, and durability of electric train traction drives, considering various factors that influence the wear and performance of gear systems.

1. The dynamic forces acting on the traction systems, such as oscillations due to track irregularities, lateral swaying, and hunting motions, cause considerable stress on the gearbox. This results in significant wear and fatigue over time, reducing the lifespan of the components.

2. Gear wear, especially when new gears are paired with worn-out wheels, increases the dynamic loads significantly. This heightened stress negatively affects the performance of the drive system.

3. The chapter utilizes finite element analysis to identify critical areas in the gearbox where stress concentrations occur, particularly at sharp transitions in geometry and surface imperfections. This analysis helps in identifying potential failure points and designing improvements to enhance durability.

CHAPTER 4. INFLUENCE OF DYNAMIC LOADS ON STRESS AND FATIGUE OF STRUCTURES

4.1. Stress of metal structure under the influence of driving forces

In the presence of a histogram representing the distribution of stress amplitude values characterizing the stress state of the part during the expected service life and the absence of parameters of the material fatigue curve, the fatigue strength assessment should be performed using the following data presented in Fig. 4.1.

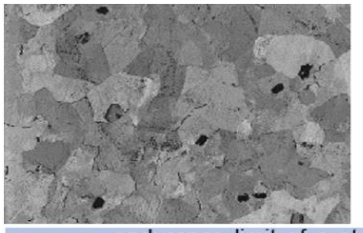

Fatigue resistance:

$$n = \frac{\sigma_{-1p}}{K_\sigma \sigma_a + \Psi_\sigma \frac{\sigma_m}{\alpha_\sigma}}$$

Endurance limit:

$$K_\sigma = \frac{K_1 K_2}{\gamma K_m} K_3$$

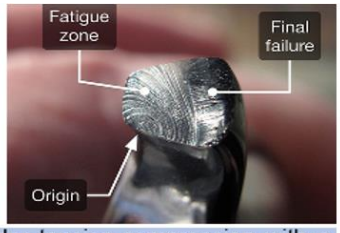

σ_{-1p} — endurance limit of a standard specimen under tension-compression with a symmetric loading cycle, for ISO 10816, $\sigma_{-1p} = 182$ MPa;

K_σ — coefficient accounting for the reduction in endurance limit of the structure compared to the endurance limit of a standard specimen (stress concentration coefficient);

σ_a — stress amplitude (maximum in the concentration zone) of the cycle, MPa;

σ_m — mean stress of the cycle, MPa;

Ψ_σ — coefficient accounting for the effect of cycle asymmetry, taken as $\Psi_\sigma = 0.3$ when $\sigma_m > 0$, and $\Psi_\sigma = 0$ when $\sigma_m < 0$;

α_σ — theoretical stress concentration factor, assumed to be 1.0.

K_1 — coefficient accounting for the influence of material heterogeneity. For rolled, forged, and stamped parts $K_1 = 1.1$, and for cast parts, $K_1 = 1.25$; .

K_2 — coefficient accounting for the influence of internal stresses in the part, dependent on the largest transverse dimension of the part. For dimensions from 250 to 1000 mm, the coefficient ranges from 1.0 to 1.2;

K_m — coefficient accounting for the surface condition of the part and depends on the machining method:

- 1.0 — for polished surfaces;
- 0.9 — for surfaces after fine machining;
- 0.8 — for surfaces after rough machining, surfaces with scale, and steel cast surfaces after sandblasting;

γ — coefficient accounting for the dimensional factor, selected depending on the largest cross-sectional size h:

- 0.8 — for section heights up to 100 mm inclusive;
- 0.75 — for section heights from 100 to 250 mm inclusive;
- 0.7 — for section heights over 250 mm;

K_3 — correction factor used for welded joint zones.

Fig. 4.1. Fatigue resistance evaluation.

To assess the maximum stresses of the MRB structure, Mode III is presented as the most severe in terms of ensuring the necessary strength parameters [29].

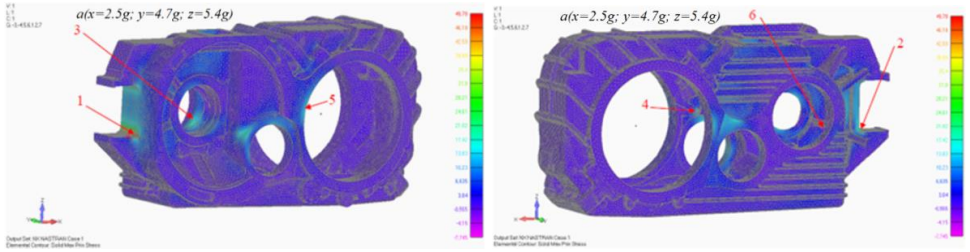

Fig. 4.2. Max principal stress [MPa] of Mode III, rotation in the forward direction.

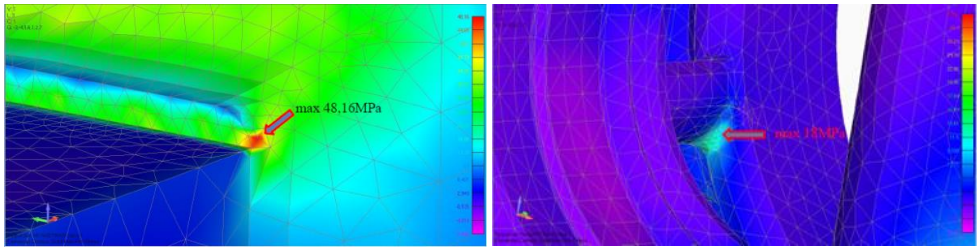

Fig. 4.3. Max principal stress [MPa] at points 1 and 6 of Mode III, rotation in the forward direction.

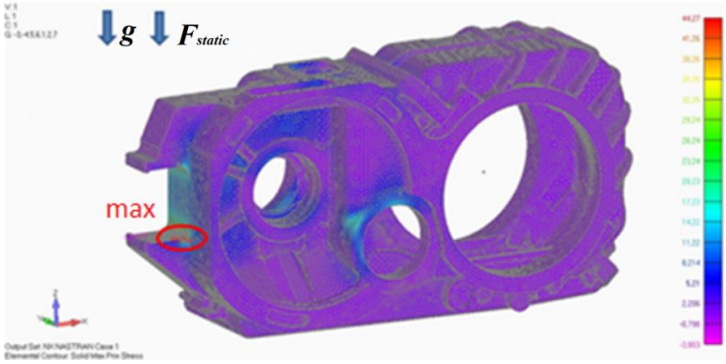

Fig. 4.4. Max principal stress [MPa] of Mode III, rotation in the forward direction.

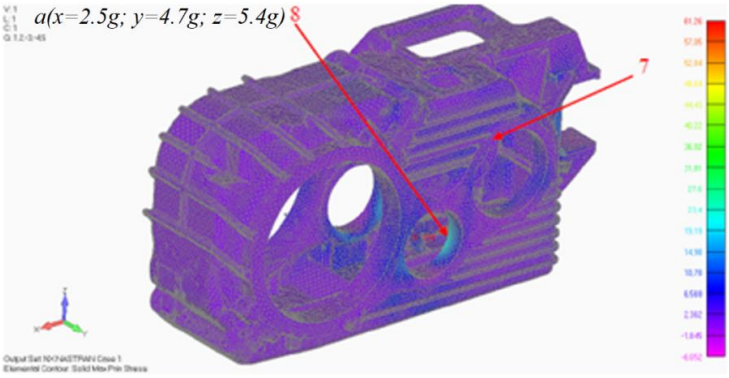

Fig. 4.5. Max principal stress [MPa] of Mode III, rotation in the reverse direction.

Table 4.1

Reverse Rotation mode. Safety Factor of Fatigue Strength

Indicator name (designation)	Values					
Stress point number (max)	1	2	3	4	5	6
(12.5; 4; 13.5) g	49.78	21.20	26.36	33.35	11.32	17.1
(–12.5; –4; –13.5) g	40.98	–3.64	4.04	22.42	–3.65	–15.8
$\sigma_m = (\sigma_{max} + \sigma_{min})/2$	45.38	8.78	15.2	27.88	3.84	0.65
$\sigma_a = \sigma_{max} - \sigma_m$	4.4	12.42	11.16	5.47	7.48	16.45
Ψ_σ	0.3	0.3	0.3	0.3	0.3	0.3
α_σ	1	1	1	1	1	1
K_σ	1.82	1.82	1.82	1.82	1.82	1.82
n	8.42	7.21	10.37	9.93	12.34	6.04

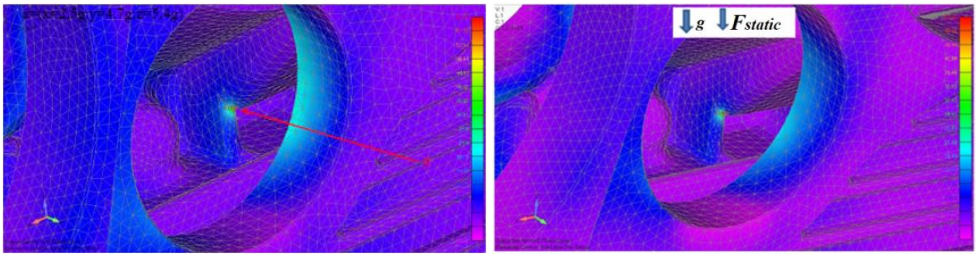

Fig. 4.6. Max principal stress [MPa] of Mode III, rotation in the reverse direction.

Table 4.2

Reverse Rotation Mode. Safety Factor of Fatigue Strength

Indicator name (designation)	Values		
Stress point number (max)	7	8	9
(12.5; 4; 13.5) g	26.4	23.4	61.26
(–12.5; –4; –13.5) g	–2	11.7	43.73
$\sigma_m = (\sigma_{max} + \sigma_{min})/2$	12.2	17.55	52.49
$\sigma_a = \sigma_{max} - \sigma_m$	14.2	5.85	8.76
Ψ_σ	0.3	0.3	0.3
α_σ	1	1	1
K_σ	1.82	1.82	1.82
n	6.16	11.44	5.75

For the calculated Mode I, the minimum allowable safety margin when calculating the strength based on allowable stresses is $[n] > 1.0$.

The minimum permissible stresses in accordance with *ISO 10816* allow the safety factors given in Table 4.3.

Table 4.3

Acceptable Stresses Values

Calculation mode	n_{min} (calculated)	$[n]$	Safety margin for the selected design
Mode III (direct rotation direction)			
1	2	8.47	acceptable
2	2	7.23	acceptable
3	2	10.6	acceptable
4	2	9.87	acceptable
5	2	12.40	acceptable
6	2	6.11	acceptable
Mode III (reverse rotation direction)			
7	2	6.19	acceptable
8	2	11.39	acceptable
9	2	5.68	acceptable

4.2. Determination of loads in elastic connecting elements

The gearbox is attached to the motor with a bolted connection. The wheel is attached with a coupling to the output shaft. The gearbox hangs on two elastic bearings on the pinion side and on rubber wedge coupling on the output shaft side. The single cardanic coupling accepts axial, radial and angular misalignments [31].

Forces from shocks acting on the gearbox in the calculation of shock forces are considered only vertical acceleration; forces from transverse and longitudinal accelerations are negligible. The general calculation scheme of the acting forces is presented in Fig. 4.7.

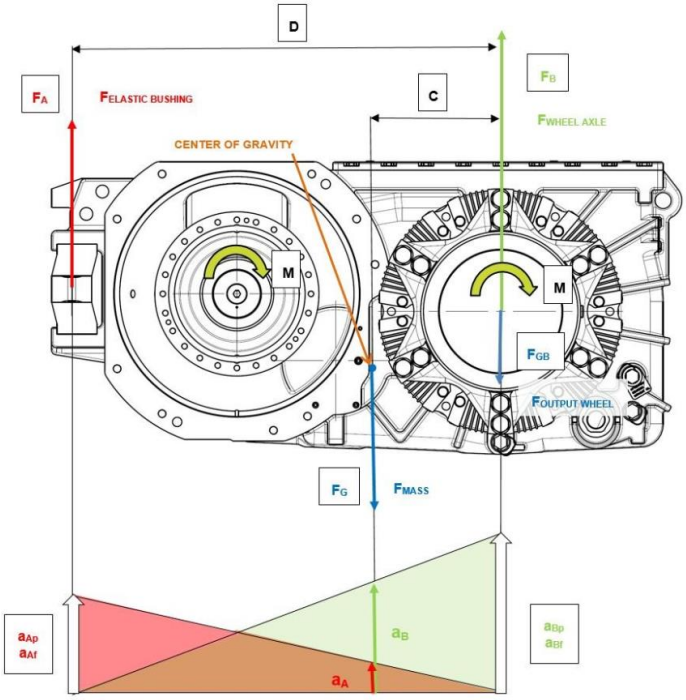

Fig. 4.7. Diagram of load distribution, where F_A is the force in elastic bushings; F_B is the force in wheel axle; and F_G is the force of gravity.

A radial displacement of 0.1575 mm is applied on hub bore diameter nodes. The corresponding total load is applied on holes for bolts in arms. The coupling assembly has to transmit an output torque of 72 580.6 Nm (input short circuit torque of 11 000 Nm). Motor tractive torque is 2 702 Nm, which corresponds to 17 828 Nm on coupling, as shown in Table 4.4.

Table 4.4

Load Parameters of Rubber Wedge Coupling

Input torque [Nm]	Ratio *i* [1]	Output Ttrque [Nm]	Diameter [mm]	Tangential force from 1 rubber wedge [N]
11 000	6.598	72 580.6	383.7	63 053
2702	6.598	17 828	383.7	15 488

Maximal overlap is used for analyses. In reality, this value is decreased by the influence of shaft and roughness.

Load case 1: Maximum von Mises stress 333 Mpa. Safety factor to yield point: 1.26.

Load case 2: Maximum von Mises stress 345 Mpa. Safety factor to yield point: 1.22.

Load case 3: Maximum von Mises stress 330 Mpa. Safety factor to yield point: 1.27.

Tractive torque has negligible influence on stress, as shown in Table 4.5 and Figs. 4.8, 4.9 and 4.10.

Table 4.5

Definition of the Safety Factor Index Relative to the Criteria

Load case	Type of analysis	Stress [Mpa]	Safety [1]	Safety criteria
LC1	static	333	To yield point: $k = \frac{420}{333} = 1.26$ To strength limit: $333\ MPa < 700\ MPa$ Strain: $\varepsilon = 0.161\ \%$	$\sigma < R_m$ $\varepsilon < 4\%$
LC2	static	345	To yield point: $k = \frac{420}{345} = 1.22$ To strength limit: $333\ MPa < 700\ MPa$ Strain: $\varepsilon = 0.161\ \%$	$\sigma < R_m$ $\varepsilon < 4\%$
LC3	fatigue	330	To yield point: $k = \frac{420}{330} = 1.27$ To strength limit: $333\ MPa < 700\ MPa$ Strain: $\varepsilon = 0.161\ \%$	Min 1.0

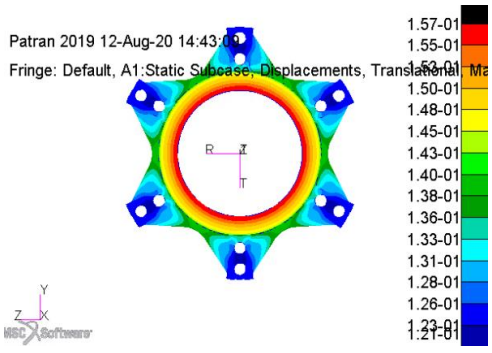

Fig. 4.8. Load case 1: maximal fit S_{max}; displacement [mm].

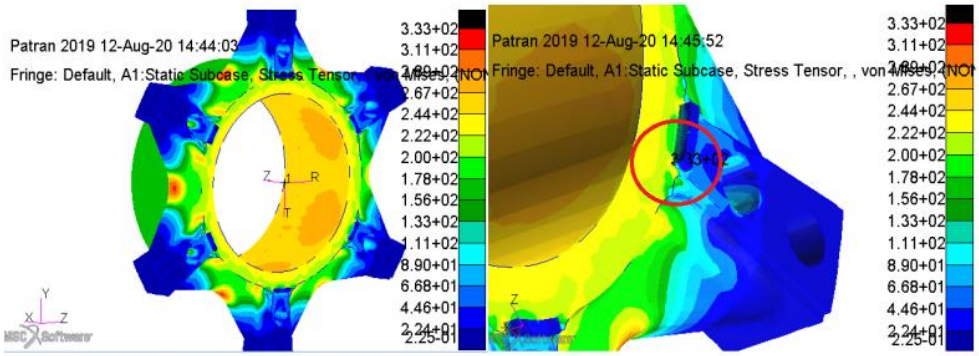

Fig. 4.9. Load case 1: maximal fit S_{max}; von Mises stress [Mpa].

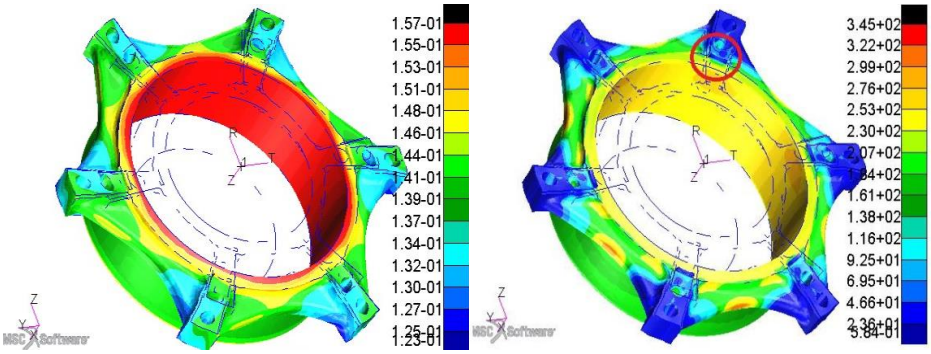

Fig. 4.10. Load case 2: maximal fit S_{max} + Short circuit torque;
a) displacement [mm]; b) von Mises stress [Mpa].

4.3. Chapter conclusions

The chapter presents an analysis of the compliance of the MGU design with the minimum permissible stresses in accordance with *ISO 10816* for permissible values of the safety factor. The determined places of maximum stress concentration are decisive for further analysis of the vibration state of the MGU with changing design and energy parameters.

It should be noted that the technology for manufacturing traction motors provides for the possibility of manufacturing frames not in the form of cast parts but in the form of charge-welded structures. This fact does not affect the applicability of the calculation method due to the use of a three-dimensional design software for both cases.

CHAPTER 5. INFLUENCE OF THE TECHNICAL CONDITION OF THE MGU ON THE VIBRATION STABILITY AND TRACTION-ENERGY CHARACTERISTICS OF THE MOTOR

5.1. Dynamic traction indicators

The running traction and energy parameters of the motor for determining the vibration activity of the MGU in the long-term mutual loading mode were determined using MATLAB/Simulink. The aim of the study is to determine the dependence of the vibration characteristics of the MGU simultaneously with the change in the energy characteristics of the motor to identify the causes of its non-compliance with the required parameters at the stage of acceptance tests.

The developed test method uses two frequency converters that perform double energy conversion. First, the voltage supplied from the network is rectified, smoothed, and then inverted to power the motors. The rectifiers are uncontrolled (diode bridge), and the inverters are controlled (IGBT transistors). Between the rectifiers and inverters there are DC links that are combined into one system. The implementation of the mutual load mode is carried out by setting different frequencies of the supply voltage on the tested electrical machines. In this case, one of the electrical machines operates in the motor mode and the other in the generator mode. The electrical energy generated by the generator is transmitted via the DC link to the motor. In this case, the energy required to compensate for losses in both machines is consumed from the network [31].

The characteristics of the traction motor, obtained experimentally, to test its own vibration in the frequency range from 20 Hz to 62 Hz correspond to those presented in Figs. 5.1–5.6.

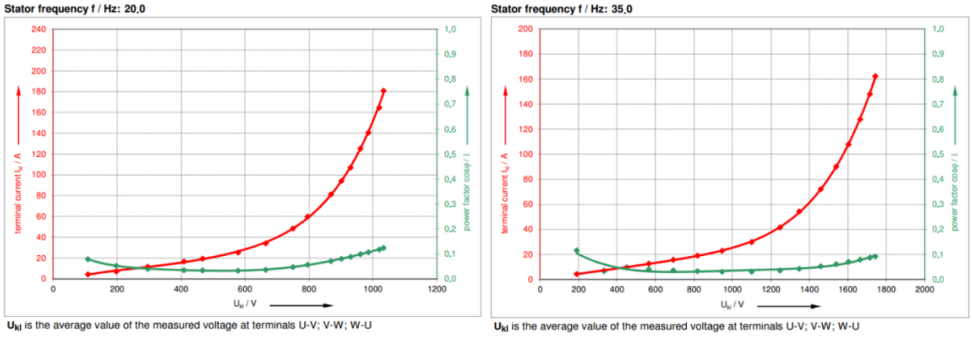

Fig. 5.1. No load test. Current and power factor versus voltage at 20 Hz and 35 Hz (*f* is the calculated average of the measured frequency values).

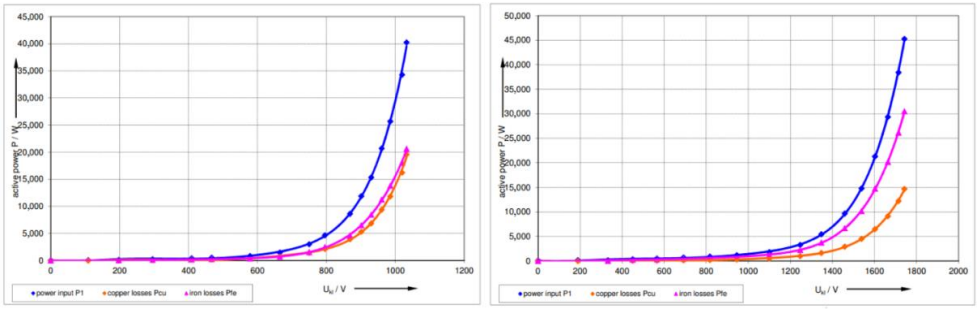

Fig. 5.2. Overview of power versus voltage at 20 Hz and 35 Hz.

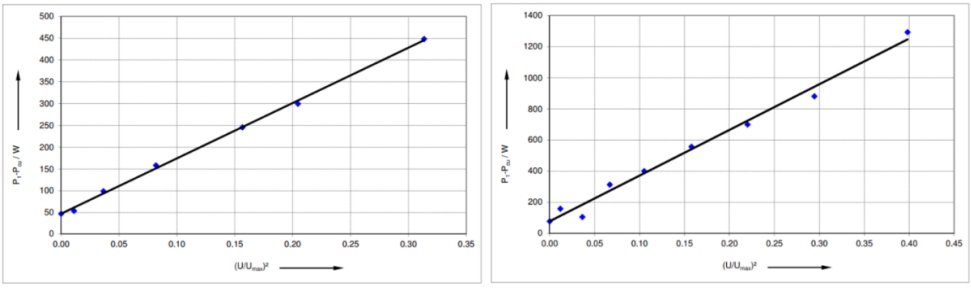

Fig. 5.3. Mechanical losses at 20 Hz and 35 Hz. The mechanical losses were determined by extrapolation of P_1-P_{Cu} at no load to 0 V. P_{mech} / W: 47 at 20 Hz point and P_{mech} / W: 77 at 35 Hz point.

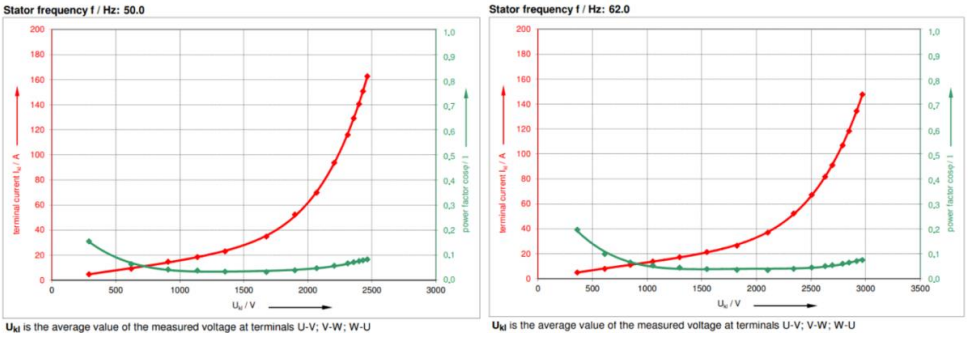

Fig. 5.4. No load test. Current and power factor versus voltage at 50 Hz and 62 Hz (*f* is the calculated average of the measured frequency values).

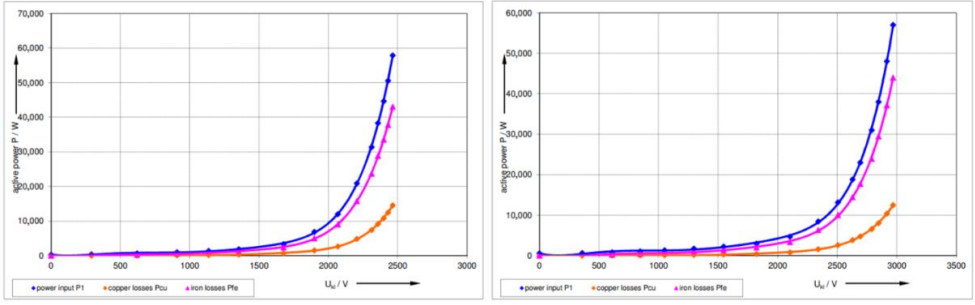

Fig. 5.5. Overview of power versus voltage at 50 Hz and 62 Hz.

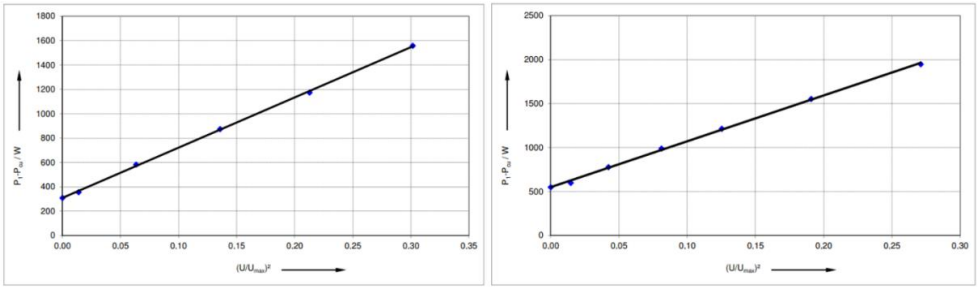

Fig. 5.6. Mechanical losses at 50 Hz and at 62 Hz. The mechanical losses were determined by extrapolation of P_1-P_{Cu} at no load to 0 V. P_{mech} / W: 308 at 50 Hz point and P_{mech} / W: 548 at 62 Hz point.

The characteristics of the traction motor, obtained experimentally to test its vibration activity and possible changes in energy characteristics under the load in the frequency range, are presented in Figs. 5.7–5.14.

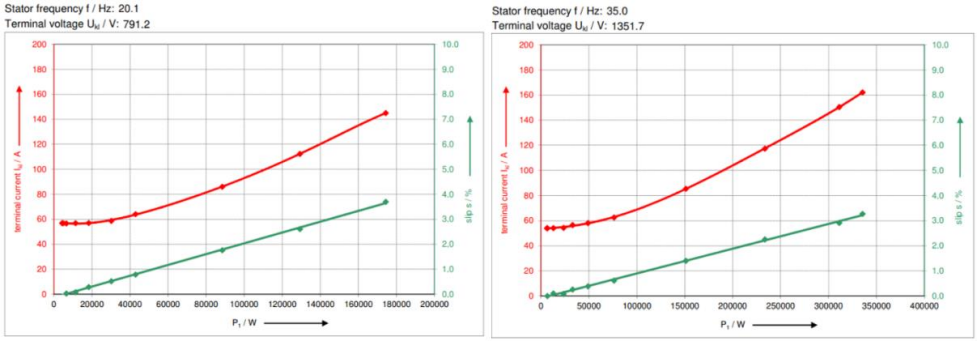

Fig. 5.7. Load characteristics. Terminal current and slip versus power at 20 Hz and 35 Hz.

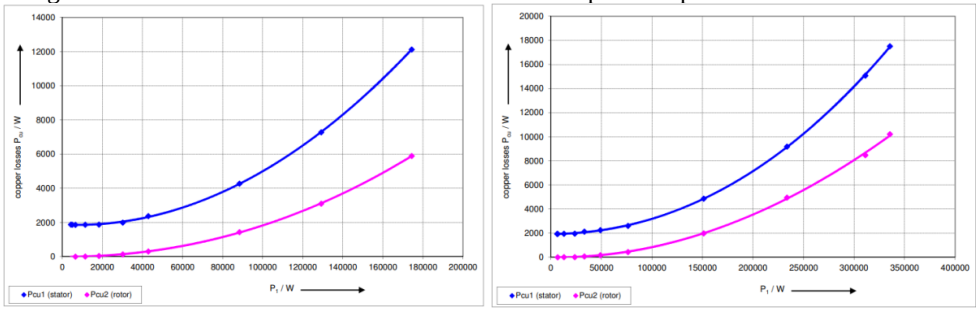

Fig. 5.8. Copper losses versus power at 20 Hz and 35 Hz.

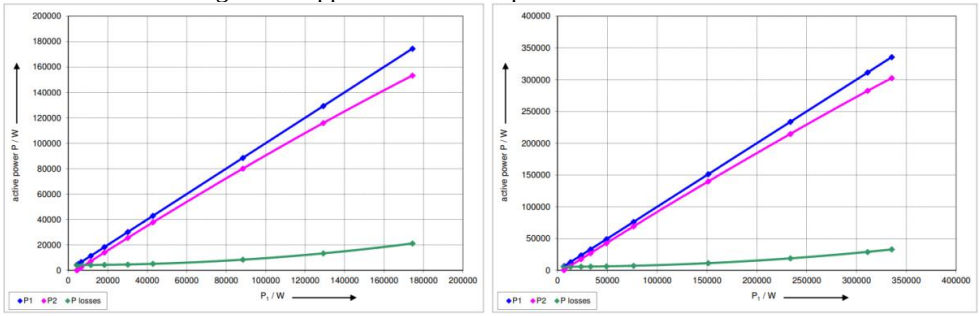

Fig. 5.9. Overview of power at 20 Hz and 35 Hz.

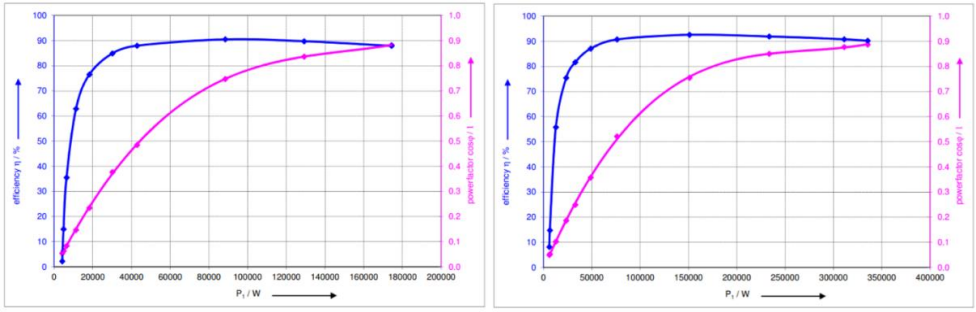

Fig. 5.10. Efficiency and power factor versus power at 20 Hz and 35 Hz.

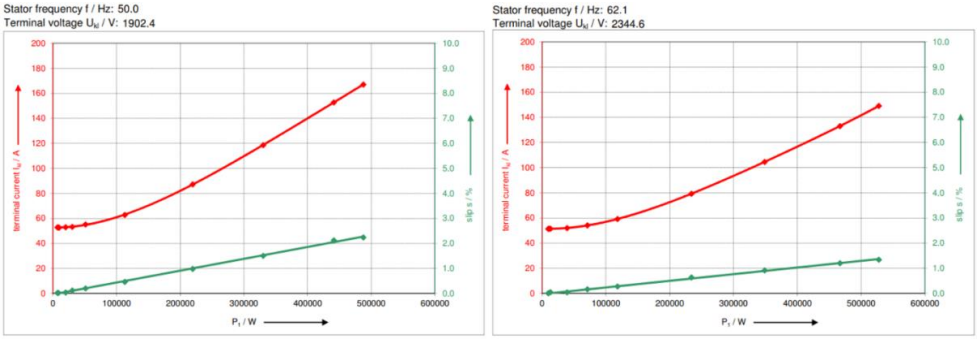

Fig. 5.11. Load characteristics. Terminal current and slip versus power at 50 and 62 Hz.

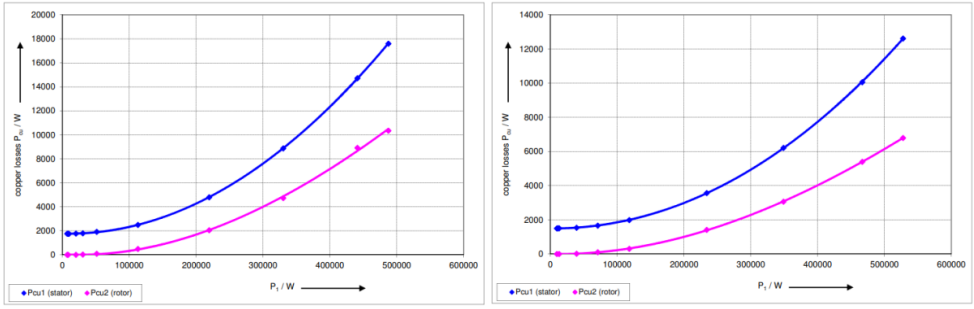

Fig. 5.12. Copper losses versus power at 50 Hz and 62 Hz.

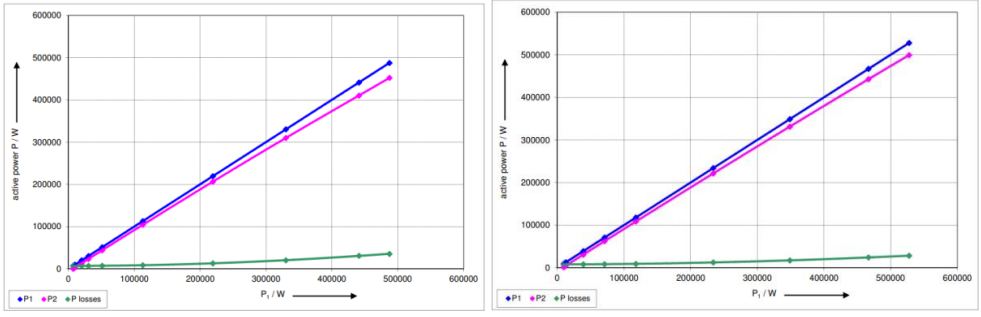

Fig. 5.13. Overview of power at 50 Hz and 62 Hz.

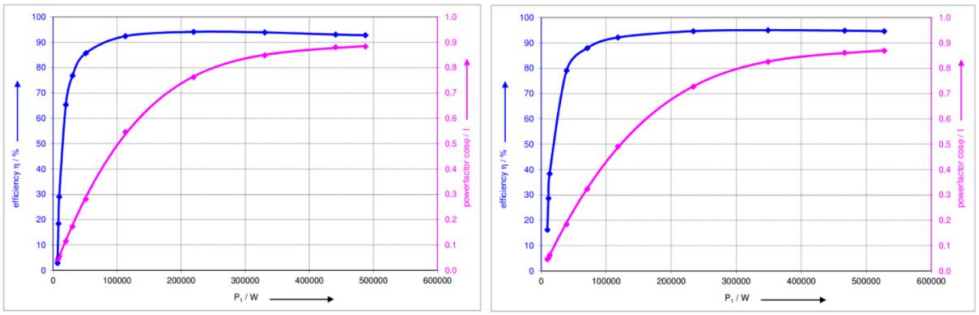

Fig. 5.14. Efficiency and power factor versus power at 50 Hz and 62 Hz.

5.2. The relationship between the causes of vibration and the diagnosed parameters

The running traction and energy parameters of the motor for determining the vibration activity of the MGU in the long-term mutual loading mode were determined using MATLAB/Simulink. The aim of the study is to determine the dependence of the vibration characteristics of the MGU simultaneously with the change in the energy characteristics of the motor to identify the causes of its non-compliance with the required parameters at the stage of acceptance tests.

The developed test method uses two frequency converters that perform double energy conversion. First, the voltage supplied from the network is rectified, smoothed, and then inverted to power the motors. The rectifiers are uncontrolled (diode bridge), and the inverters are controlled (IGBT transistors). Between the rectifiers and inverters there are DC links that are combined into one system. The implementation of the mutual load mode is carried out by setting different frequencies of the supply voltage on the tested electrical machines. In this case, one of the electrical machines operates in the motor mode and the other in the generator mode. The electrical energy generated by the generator is transmitted via the DC link to the motor. In this case, the energy required to compensate for losses in both machines is consumed from the network.

Two identical MGUs are used simultaneously during testing. Frequency converters are used as a control link instead of additional electric machines. Electric energy is transferred directly to the MGU under test and compared to circuits that provide electric energy transfer to the network, which reduces the impact of higher harmonics of currents and voltages on the network.

Reciprocal load implementation is possible at any difference in the supply voltage frequencies set on the frequency converters, in contrast to testing at industrial voltage frequency.

In accordance with *ISO 10816*, as part of the mechanical stability check of the product, it is advisable to conduct an autonomous check of the traction motor to determine its own vibration activity for at least one of the quantities specified in the standard [31]:

- vibration displacement, in micrometres (μm);
- vibration velocity, in millimetres per second (mm/s);
- vibration acceleration, in metres per second squared (m/s^2).

According to *ISO 10816*, the maximum measurable vibration level is up to 5 mm/s in the direction transverse to the output shaft and 2.5 mm/s in the direction along the output shaft.

All components must withstand vibration and impacts, sinusoidal vibration with a maximum acceleration amplitude of 150 m/s^2 in the frequency range of 0.5–100 Hz without damage.

It is assumed that the specified impact is exerted from the wheelset on the wedge clutch [32].

The test cycle and the completeness of the laboratory equipment are shown in Fig. 5.15.

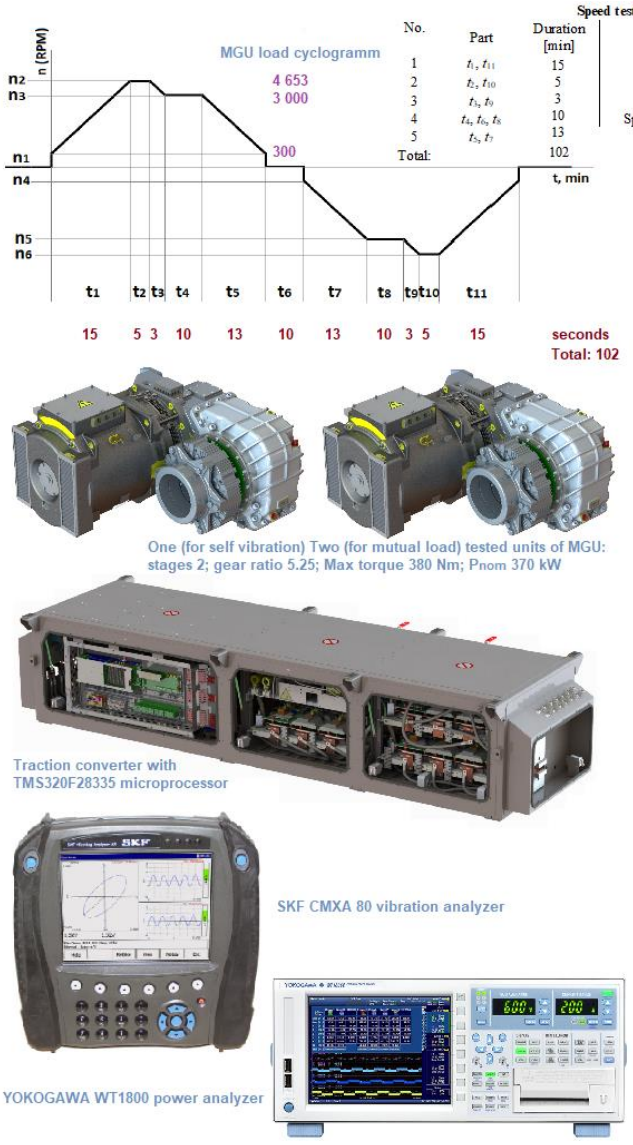

Fig. 5.15. The test cycle and the completeness of the laboratory equipment [26].

Further, Figs. 5.16 and 5.17 show the vibration acceleration spectra for the nominal rotation speed of the MGU equal to 3000 min^{-1} in the idle mode, with the MGU mechanically

disconnected and in the mutual load mode. It is evident that the vibration disturbance characteristic clearly repeats the MGU loading cyclogram in the modulus shown in Fig. 5.15.

The spectral analysis results were obtained using the fast Fourier transform. The decomposition of the vibration signature leads to motor speed-dependent orders, speed-independent components, and speed-related non-zero harmonics. The last two components are due to the inverter [32].

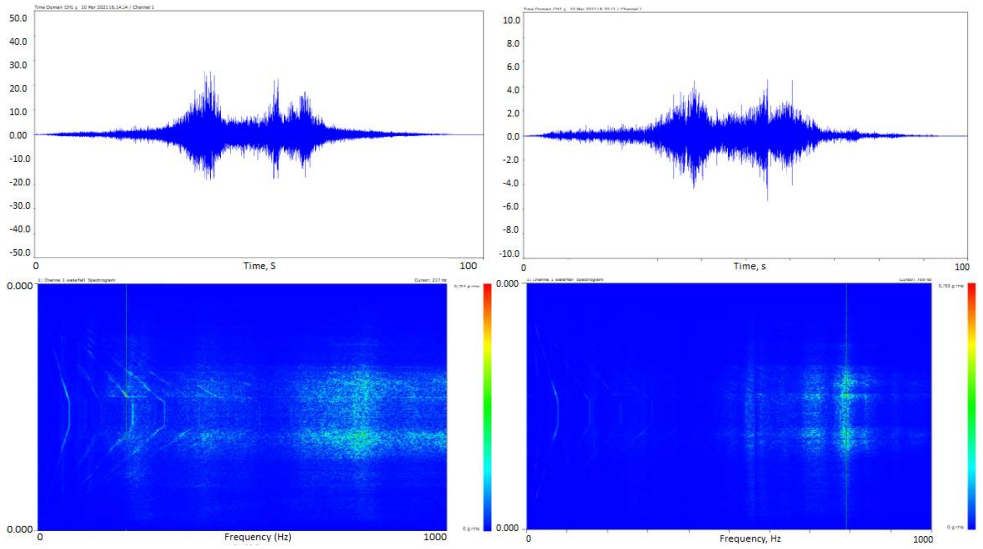

Fig. 5.16. The waveform and waterfall spectrogram at the rotor speed of nominal velocity 3000 min^{-1} in the Y-axis direction (left side) without load and in mutual load mode (right side).

At the same time, in the coasting mode, the possible presence of resonance can be determined. Fig. 5.17 shows a distinct resonance of the traction motor when the rotor speed is within the limited construction speed and at the rated speed.

For a rotation speed of 3000 min^{-1}, in the range of 50.0...100.0 Hz (step 1.75 Hz), an increase in the RMS vibration speed up to 40 mm/s in the direction of the Y-axis is fixed. For a maximal rotation speed of 4653 min^{-1}, in the range of 50.0...75.0 Hz (step 1.75 Hz), the situation has worsened, with an increase in the RMS vibration speed up to 50 mm/s, in the direction of the Y-axis, was fixed. For the assumptions put forward in the previous chapters about the role of the geometry of the bearing mounting holes in the shield and the coaxiality of the intermediate flange of the MGU and the bearing cite, the MGU was disassembled. As a result of determining the possible causes of increased vibration, a violation of the technology for processing the bearing shield and the flange of the MGU was revealed in terms of the displacement of the centres of both elements [33].

At the same time, the energy parameters were recalculated relative to the oscillograms recorded by the converter; they can be seen in Figs. 5.18 and 5.19.

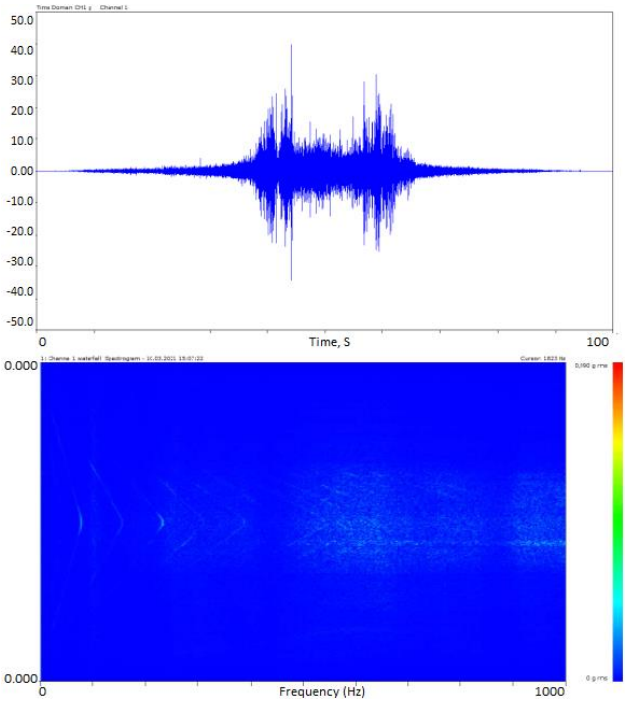

Fig. 5.17. The waveform of the vibration velocity at a continuous speed of 3000 min^{-1}.

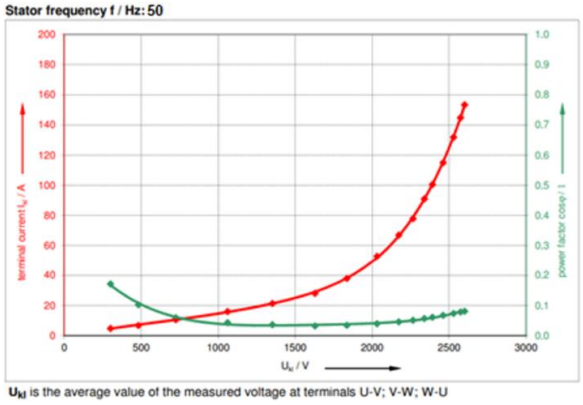

Fig. 5.18. No load test. Current and power factor versus voltage at 50 Hz.

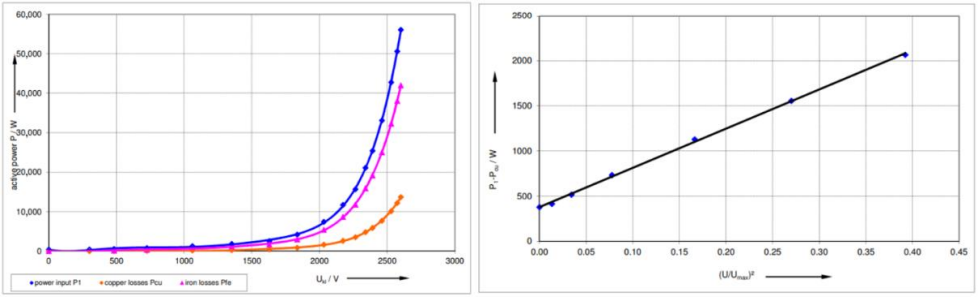

Fig. 5.19. Overview of power versus voltage and mechanical losses at 50 Hz. The mechanical losses were determined by extrapolation of P_1-P_{Cu} at no load to 0 V. P_{mech} / W: 378.

The vibration velocity values recorded during the experiment in the direction of the Y-axis, i.e., along the shaft axis, are several times higher than the values, the limit of which is specified in *ISO 10816* at 2.8 mm/s, both for the nominal and maximum value of rotor rotation. In addition to the given values, the vibration activity level of the MGU was recorded at 21 points and in three planes, both from the side of the motor support shield and from the side of the 1st stage bearing of the traction gearbox.

In an asynchronous motor, the speed is inversely proportional to the load, but when it is transmitted through a gearbox, a certain speed fluctuation is observed. When the rotational speed of the MGU rotor-shaft system increases from 3000 min^{-1} to 4653 min^{-1}, the vibration velocity values at the control points increase.

Vibration activity of the middle gears of the gear is less informative due to the fact that it can be caused by an obvious defect of the gear mechanism of the gear, such as misalignment or defects of the contact surface. In turn, the consequence of most defects is impacts of surfaces against each other or pulsed jumps in the load on the elements transmitting the torque to the driven shaft (rotor). Then, the load jumps are transmitted to the bearings of the mechanical transmission and excitation of pulse vibration in them.

The description of the load and possible wear options for the bearing mounting holes given in Chapters 3 and 4, and the resulting changes in the energy parameters of the motor, can be better represented by the misalignment of the motor bearing shield and the flange connecting the motor and gearbox.

The level of vibration activity is fixed on the Y-axis, so it is reasonable to assume the action of tangential forces arising in the MMF [33], [34].

A feature of the action of oscillatory forces of both electromagnetic and electrodynamic nature is their spatial wave character. In defect-free motors, the oscillatory forces (radial and tangential) acting on the rotor are zero. The tangential electrodynamic forces acting on the stator are also zero. Low-order electromagnetic radial oscillatory forces bend the stator, creating a wave of radial oscillations of double frequency and double spatial order.

The reliability of the electromagnetic system of the motor depends on the symmetry of the magnetic field, determined by the symmetry of the windings, the symmetry of the air gaps between the rotor and the stator, the equality of the magnetomotive forces of the windings, as well as on the state of fastening of the machine elements and the insulation of the electrical windings. Asymmetry of air gaps in the motor leads to the appearance of electromagnetic forces between the rotor and stator in the area of reduced gap, overloading the bearings and reducing their service life, and in the same area, magnetic saturation of the magnetic circuit teeth occurs, along which the magnetic flux bypasses the turns of the electric motor winding. The vibration level is manifested at the frequency of electromagnetic forces and at the frequency of rotation of the magnetic field in the gap. Figs. 5.20 and 5.21 show the general appearance of the MGU device on a platform with a spring suspension.

The magnitude of the components of the vibrations of the MGU depends on the magnitude of the oscillatory forces and on the rigidity of the oscillatory system. Large oscillatory forces are electromagnetic, which act between the rotor and the stator in the radial direction, i.e., bend the machine body in accordance with the complex spatial shape of the magnetic field. The shape of the magnetic field and the deformation of the stator have angular symmetry and are characterized by the order of oscillations, which is equal to the number of spatial waves that fit on the length of the circumference of the motor stator.

Fig. 5.20. MGU placement on the test platform to determine its own vibration.

When the electromagnetic system is defective, an asymmetry of the magnetic field in the air gap occurs, and first-order magnetic forces begin to act, shifting the rotor relative to the stator. Such a shift leads to the fact that the axial forces, trying to return the rotor to the neutral position, cause significant axial vibration at the frequency of the power supply network or at the frequency of rotation of the rotor, depending on the type of friction in the obstacle to axial displacement.

Fig. 5.21. MGU placement on the test platform under mutual load.

For the case of mutual loading, the resulting power, losses, power factor and efficiency of the drive were also obtained by oscillography, which can be seen in Figs. 5.22 and 5.23.

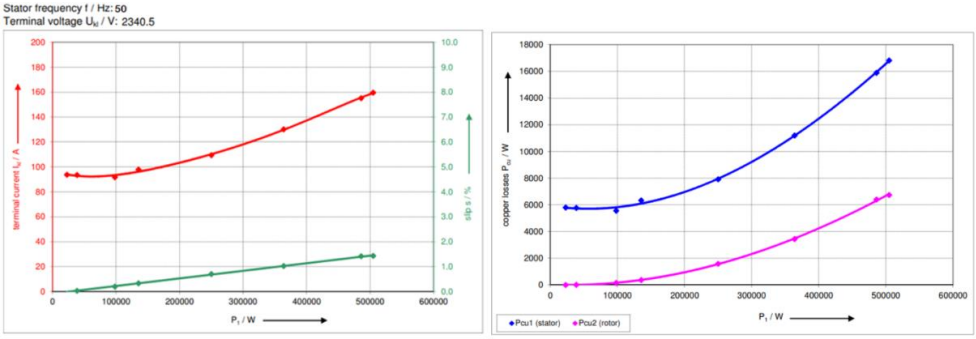

Fig. 5.22. Load characteristics. Terminal current and slip versus power and copper losses versus power at 50 Hz.

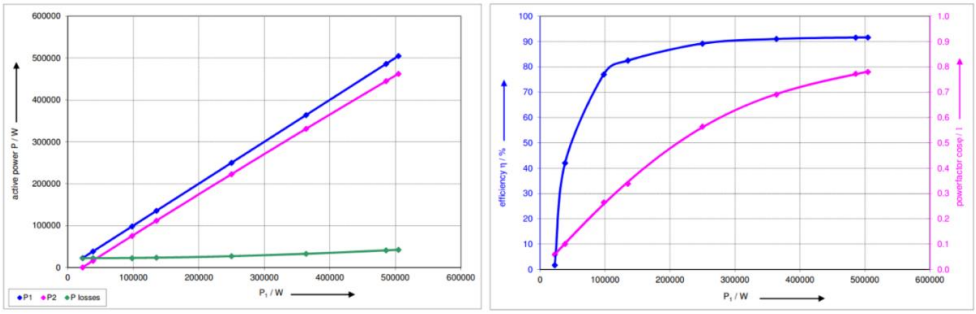

Fig. 5.23. Overview of efficiency and power factor versus power at 50 Hz.

It is evident that with the increase of the vibration velocity value in the vertical direction Y, when measuring it on the bearing shield and the flange of the MGU in the idle mode, under load, and also, which is most informative, in the rotor run-out mode, the influence of the misalignment of the MGU support structures, the shaft displacement relative to the axis and, as a consequence, there is the change of the air gap. From the conducted study, it is evident that the change of the air gap uniformity is most negatively expressed in the increase of mechanical losses and the decrease of slip, more than 10 % decrease in the power factor of the drive, and together with it the efficiency of the drive as a whole. The purpose of the study was to determine the possibility of using the MGU vibration activity indicator, which is a mandatory parameter when conducting acceptance tests of traction MGUs, as the main rejection feature, and taking into account the nature of the manifestation of vibration activity and its value – then as a determinant of poor quality of the MGU parts or its assembly.

RESULTS AND CONCLUSIONS

The Doctoral Thesis examines the possibilities of assessing the technical condition and readiness for the release of serially produced MGUs based on vibration strength tests and traction and energy indicators. When setting the tasks of the Thesis research, there was a requirement to implement the methodology in the flow production of the manufacturing enterprise and the adaptability of the methodology to the product line, and not to one specific product.

During the implementation of the methodology in production, about a hundred motor-gear units for rail transport were produced, which simultaneously increased its reliability during acceptance tests.

The developed methodology is based on the real features of the technological process of production, as well as on the real operating conditions of the equipment, considering the mechanical loads of the traction drive.

To determine the possible influence of electromagnetic phenomena from the traction drive on the vibration strength characteristics of the MGU with a subsequent change in the traction and energy parameters of the motor, a strength calculation of the structure was carried out with the definition of critical areas of maximum stresses, the safety margin of the structure was determined. The experiment determined the level of vibration activity of the MGU in a loaded mode.

The methodology was tested both on a reference MGU sample and on a sample that does not meet the requirements of the Technical Specifications of the product.

Thus, for MGUs, in which the geometry of the electric motor flange and the bearing shield ensures both the average position of the motor roller bearing, which is most favourable in terms of reducing vibration activity and the average position of the rotor and its symmetrical arrangement, a number of patterns have been established.

The determining factor in monitoring the traction-energy and vibration-resistant parameters of the MGU is the dynamics of the change in the vibration velocity level, and as a consequence, deterioration of slip, increase in mechanical losses, and a significant decrease in the power factor and efficiency. It has been established that vibration is continuous in time and corresponds to the spectrum of the broadband region.

A number of key regulatory documents prescribe monitoring of the overall vibration level in a standard frequency band – from 10 Hz to 1000 Hz. However, in most cases, one or more fault frequencies (frequencies at which vibration growth indicates the presence or development of a particular defect) are outside the monitored frequency range. Thus, even a significant increase in the amplitudes of the components at these frequencies does not lead to a change in the overall vibration level in the standard frequency band monitored in accordance with the requirements of regulatory documents. Faults that occur at frequencies outside the frequency range under consideration include a number of electromagnetic defects, such as air gap eccentricity, gear defects, etc.

The value of the overall vibration level is quite informative but characterizes the combined vibration activity of all the main components of the monitored unit – the degree of "balance" of the rotors, the quality of the alignment, the state of the support system, etc. Some defects do not always lead to a noticeable increase in the overall vibration level. To prevent emergency failures

and timely detection of these types of faults, along with monitoring the general level, it is necessary to analyze the vibration velocity spectrum measured in the transverse direction and in the vertical direction.

This study is a continuation of the study of the vibration activity of rotating electric machines and traction units, as the most information-intensive characteristic throughout the entire service life of the product during routine inspections and repair and restoration work of the rolling stock.

From the point of view of economic feasibility, it can be highlighted that the end customer of the drive is most often a wagon-building company, much less often a repair company, interested in receiving an already tested and ready-to-install product, preferably from one manufacturer, which significantly reduces the time, and accordingly, the cost of commissioning and running tests of electric trains. The proposed method for determining the causes of a malfunction of the MGU is focused specifically on the complete supply of an electric traction drive.

LIST OF REFERENCES

1. Holopainen, T. P., Niiranen, J., Jörg, P., Andreo, D. “Electric Motors and Drives in Torsional Vibration Analysis and Design”, Proceedings of the Forty-Second Turbomachinery Symposium, Houston, Texas, October 1-3, 2013.
2. Paul de Vos. “Railway Induced Vibration – State of the Art Report”, UIC-ETC (Railway Technical Publications), 2017.
3. Zhang, T., Jin, T., Zhou, Z., Chen, Z., Wang, K. “Dynamic modeling of a metro vehicle considering the motor–gearbox transmission system under traction conditions”, Mech. Sci., 13, 603–617, https://doi.org/10.5194/ms-13-603-2022, 2022.
4. ISO 13373-1:2002 – Condition monitoring and diagnostics of machines – Vibration condition monitoring – Part 1: General procedures, Edition 1, 2002.
5. ISO 15242-1:2015 – Rolling bearings – Measuring methods for vibration – Part 1: Fundamentals, Edition 2, 2015.
6. GOST 24346-80 – Vibration Terms and definitions, Moscow Standartinform, 2010.
7. ISO 20816-3:2022 – Mechanical vibration – Measurement and evaluation of machine vibration. Part 3: Industrial machinery with a power rating above 15 kW and operating speeds between 120 r/min and 30 000 r/min, Edition 1, 2022.
8. ISO 13379-1:2012 – Condition monitoring and diagnostics of machines – Data interpretation and diagnostics techniques. Part 1: General guidelines, Edition 1, 2012.
9. ISO 13379-2:2015 – Condition monitoring and diagnostics of machines – Data interpretation and diagnostics techniques. Part 2: Data-driven approach, Edition 1, 2015.
10. Nabhan, A., Nouby, M., Sami, A. M., Mousa, M. O. “Bearing fault detection techniques – a review”, Turkish Journal of Engineering, Sciences and Technology, 2015.
11. Wang, X., Peng, T. F., Wu, P. B., Cui, L. T. “Influence of electrical part of traction transmission on dynamic characteristics of railway vehicles based on electromechanical coupling model”, Scientific Reports, Volume 11, 2021.
12. Wang, H., Núñez, A., Liu, Z., Zhang, D., Dollevoet, R. “A Bayesian network approach for condition monitoring of high-speed railway catenaries”, Transactions on Intelligent Transportation Systems, Volume 21, 2020.
13. Wang, B., Xie, S., Jiang, C., Song, Q., Sun, S., Wang, X. “An investigation into the fatigue failure of metro vehicle bogie frame”, Engineering Failure Analysis, Volume 118, 2020.
14. Wu, Q., Wang, B., Spiryagin, M., Cole, C. “Curving resistance from wheel-rail interface”, Vehicle System Dynamics, Volume 60, Issue 3, 2020.
15. Mao, L., Wang, W. J., Liu, Z., Yang, G., Song, C., Qu S. “Research on causes of fatigue cracking in the motor hangers of high-speed trains induced by current Buctuation”, Engineering Failure Analysis, 2021.
16. Wang, Z., Yin, Z., Allen, P., Wang, R., Xiong, Q., Zhu, Y. “Dynamic analysis of enhanced gear transmissions in the vehicle-track coupled dynamic system of a high-speed train”, International Journal of Vehicle Mechanics and Mobility, Volume 60, Issue 8, 2022.
17. Wang, Z., Cheng, Y., Mei, G., Zhang, W., Huang, G., Yin, Z. “Torsional vibration analysis of the gear transmission system of high-speed trains with wheel defects”, Proceedings of the Institution of Mechanical Engineers – Part F: Journal of Rail and Rapid Transit, 2019.

18. Bogdevičius, M., Karpenko, M., Bogdevičius, P. “Determination of rheological model coefficients of pipeline composite material layers based on spectrum analysis and optimization”, Journal of Theoretical and Applied Mechanics, 2021.
19. Touhami, O., Noureddine, L., Ibtiouen, R., Fadel, M. “Modeling of the induction machine for the diagnosis of rotor defects. Part II. Simulation and experimental results”, IEEE Industrial Electronics Society, 2005.
20. Баннов, Д. “Метод диагностики обрывов стержней ротора в асинхронных электродвигателях на основе регрессионного анализа модуля результирующего вектора тока статора”, Известия Томского политехнического университета, Инжиниринг георесурсов, 2022.
21. Mazur, D., Trojnar, M. “Modelling of electrical and mechanical phenomena in induction motors with air-gap eccentricity”, Renewable Energy and Power Quality Journal, 2003.
22. Хоменко, А. “Разработка системного метода управления вибрационным состоянием подвижного состава”, Иркутск, 2000.
23. Goolak, S., Liubarskyi, B., Lukoševičius, V., Keršys, R., Keršys, A. “Operational Diagnostics System for Asymmetric Emergency Modes in Traction Drives with Direct Torque Control”, Applied Sciences, 2023.
24. Вульфсон, И. “Краткий курс теории механических колебаний”, Библиотека ВНТР, 2017.
25. Куцубина, Н., Санников, А. “Теория виброзащиты и акустической динамики машин”, Учебное пособие, Министерство образования и науки РФ, Урал. гос. лесотехн. ун-т. – Екатеринбург, 2014.
26. Dvornikov, I., Marinbahs, M., Kobenkins, G., Sliskis, O., Ketners, K. “Carrying Out of Tests for the Functionality of the Traction Autonomous Drives in the Conditions of Industry and Serial Production”, 17th Conference on Electrical Machines, Drives and Power Systems (ELMA), Bulgaria, 2021.
27. Kobenkins, G., Marinbahs, M., Burenin, V., Zarembo, J., Bizans, A., Sliskis, O. “Determination of the Level of Own Vibration of Geared Motor Boxes in Industrial Conditions” IEEE 62nd International Scientific Conference on Power and Electrical Engineering of Riga Technical University (RTUCON), Latvia, 2021.
28. Kobenkins, G., Marinbahs, M., Bizans, A., Rilevs, N., Burenin, V., Sliskis, O. “Carrying Out of Strength Control of Mutual Loaded Traction Geared Motor Boxes as a Part of Industrial Tests”, 9th International Conference on Electrical and Electronics Engineering (ICEEE), Turkey, 2022.
29. WIKOV MGI // EG2Tv 08-805209-01, Calculation of the strength of the gearbox housing, Hronov, 2019, p. 49.
30. Ehya, H., Lyng Rødal, G., Nysveen, A., Nilssen, R. “Condition Monitoring of Wound Field Synchronous Generator under Inter-turn Short Circuit Fault utilizing Vibration Signal”, 23rd International Conference on Electrical Machines and Systems (ICEMS), Hamamatsu, Japan, 2020.
31. Sharma, V. “A Review on Vibration-Based Fault Diagnosis Techniques for Wind Turbine Gearboxes Operating Under Nonstationary Conditions”, Journal of The Institution of Engineers, 2021.
32. Dvornikov, I., Marinbahs, M., Sliskis, O., Ketners, K. “Investigation of autonomous traction motor dynamic using the method of mutual loading and computer simulation”,

IEEE 59th International Scientific Conference on Power and Electrical Engineering of Riga Technical University (RTUCON), Latvia, 2018.
33. Marinbahs, M., Kobenkins, G., Pavelko, V. Bizans, A., Rilevs, N., Sliskis, O. “Determination of the Strength Characteristics of Traction Gears Under Shock Loads”, International Youth Conference on Energy (IYCE-2022), Hungary, 2022.
34. Gierlak, P., Burghardt, A., Szybicki, D., Szuster, M., Muszynska, M. “On-line manipulator tool condition monitoring based on vibration analysis”, Mechanical Systems and Signal Processing, Volume 89, 2017.

Genādijs Kobenkins was born in 1996 in Riga. He obtained a Bachelor's degree in Electrical Engineering (2018), a qualification of an engineer in Power Engineering and Electrical Engineering (2019), and a Master's degree in Power Engineering and Electrical Engineering (2020) from Riga Technical University. Since 2018, he has been a design engineer in the Electrical Machines office at JSC "Riga Electrical Machinery Factory". Since 2021, he has been a Scientific Assistant at Riga Technical University. He has participated in several scientific conferences and symposia, where he presented the latest research in the field of electrical machine vibrations. His scientific interests are related to the discovery and solution of problems in the design, testing and operation of electrical machines.